This article is a *Plant Cell* Advance Online Publication. The date of its first appearance online is the official date of publication. The article has been edited and the authors have corrected proofs, but minor changes could be made before the final version is published. Posting this version online reduces the time to publication by several weeks.

STM/BP-Like KNOXI Is Uncoupled from ARP in the Regulation of Compound Leaf Development in *Medicago truncatula*[C][W][OPEN]

Chuanen Zhou,[a,b,1] Lu Han,[c,1] Guifen Li,[d] Maofeng Chai,[a] Chunxiang Fu,[a] Xiaofei Cheng,[d] Jiangqi Wen,[d] Yuhong Tang,[d] and Zeng-Yu Wang[a,2]

[a] Forage Improvement Division, The Samuel Roberts Noble Foundation, Ardmore, Oklahoma 73401
[b] Key Laboratory of Plant Cell Engineering and Germplasm Innovation, Ministry of Education, School of Life Science, Shandong University, Jinan, Shandong 250100, P.R. China
[c] School of Medical and Life Science, University of Jinan, Jinan, Shandong 250022, P.R. China
[d] Plant Biology Division, The Samuel Roberts Noble Foundation, Ardmore, Oklahoma 73401

Class I *KNOTTED*-like homeobox (*KNOXI*) genes are critical for the maintenance of the shoot apical meristem. The expression domain of *KNOXI* is regulated by *ASYMMETRIC LEAVES1/ROUGHSHEATH2/PHANTASTICA* (*ARP*) genes, which are associated with leaf morphology. In the inverted repeat-lacking clade (IRLC) of Fabaceae, the orthologs of *LEAFY* (*LFY*) function in place of *KNOXI* to regulate compound leaf development. Here, we characterized loss-of-function mutants of *ARP* (*PHAN*) and *SHOOTMERISTEMLESS* (*STM*)- and *BREVIPEDICELLUS* (*BP*)-*like KNOXI* in the model IRLC legume species *Medicago truncatula*. The function of *ARP* genes is species specific. The repression of *STM/BP-like KNOXI* genes in leaves is not mediated by *PHAN*, and no suppression of *PHAN* by *STM/BP-like KNOXI* genes was observed either, indicating that *STM/BP-like KNOXI* genes are uncoupled from *PHAN* in *M. truncatula*. Furthermore, comparative analyses of phenotypic output in response to ectopic expression of *KNOXI* and the *M. truncatula LFY* ortholog, *SINGLE LEAFLET1* (*SGL1*), reveal that *KNOXI* and *SGL1* regulate parallel pathways in leaf development. We propose that *SGL1* probably functions in a stage-specific manner in the regulation of the indeterminate state of developing leaves in *M. truncatula*.

INTRODUCTION

KNOTTED-like homeobox (KNOX) proteins regulate both embryonic and postembryonic development in plants. *KNOX* genes fall into two subclasses, Class I *KNOX* (*KNOXI*) and Class II *KNOX* (*KNOXII*) based on sequence similarity, gene structure, and expression pattern (Hay and Tsiantis, 2010). *KNOXI* genes, which are evolutionarily close to maize (*Zea mays*) *KN1* (Vollbrecht et al., 1991), are expressed in the shoot apical meristem (SAM) of both monocot and eudicot plants and play crucial roles in the maintenance of SAM and regulation of leaf complexity across vascular plants (Long et al., 1996; Hake et al., 2004; Barkoulas et al., 2008; Hay and Tsiantis, 2010). *KNOXII* genes display diverse expression patterns, and their function is not clear (Serikawa et al., 1997; Byrne et al., 2002).

The *KNOXI* gene family from *Arabidopsis thaliana* consists of *SHOOTMERISTEMLESS* (*STM*), *BREVIPEDICELLUS* (*BP*)/*KNOTTED-like in A. thaliana 1* (*KNAT1*), *KNAT2*, and *KNAT6* (Lincoln et al., 1994; Long et al., 1996). *STM* is expressed during early embryogenesis and marks the entire SAM. The loss-of-function *stm* mutant failed to establish the SAM during embryogenesis (Long et al., 1996; Belles-Boix et al., 2006). *BP* contributes redundantly with *STM* to SAM maintenance (Byrne et al., 2002; Venglat et al., 2002), and loss of *BP* plants showed a mildly dwarfed phenotype. *KNAT2* and *KNAT6* showed redundant and antagonistic roles with *KNOXI* genes (Belles-Boix et al., 2006; Ragni et al., 2008). In the SAM, KNOXI proteins increase the cytokinin (CK) level by activating the expression of the CK biosynthesis gene *ISOPENTENYL TRANSFEREASE7* and decrease the gibberellic acid level by inhibiting the *GA 2-oxidase1* gene (Sakamoto et al., 2001; Jasinski et al., 2005; Yanai et al., 2005; Bolduc and Hake, 2009). Such high CK–low gibberellic acid conditions are required for the SAM to maintain its activity. Ectopic expression of *KNOXI* genes significantly altered leaf development (Lincoln et al., 1994; Belles-Boix et al., 2006; Shani et al., 2009). In simple-leafed species, such as *Arabidopsis*, a lobed leaf margin was observed in transgenic plants overexpressing *KNOXI*. However, in compound-leafed species, overexpression of *KNOXI* genes dramatically increased the degree of leaflet reiteration (Hareven et al., 1996; Hay and Tsiantis, 2006).

A *MYB* transcription factor, *ASYMMETRIC LEAVES1* (*AS1*) in *Arabidopsis*, *ROUGH SHEATH2* (*RS2*) in maize, and *PHANTASTICA* (*PHAN*) in *Antirrhinum majus* (together known as *ARP* factors) is a negative regulator of *KNOXI* genes (Waites et al., 1998; Timmermans et al., 1999; Tsiantis et al., 1999; Byrne et al., 2000; Guo et al., 2008; Lodha et al., 2013). Leaf forms can be classified into two major types: simple leaves and compound leaves. A simple leaf has a single unit of undivided blade, and a compound leaf consists of multiple discontinuous blades. The ARP-KNOXI regulatory module is well established in simple-leafed species. In *Arabidopsis*, a mutually exclusive expression pattern is observed between *AS1* and *STM* in the shoot apex. *STM* represses *AS1*

[1] These authors contributed equally to this work.
[2] Address correspondence to zywang@noble.org.
The author responsible for distribution of materials integral to the findings presented in this article in accordance with the policy described in the Instructions for Authors (www.plantcell.org) is: Zeng-Yu Wang (zywang@noble.org).
[C] Some figures in this article are displayed in color online but in black and white in the print edition.
[W] Online version contains Web-only data.
[OPEN] Articles can be viewed online without a subscription.
www.plantcell.org/cgi/doi/10.1105/tpc.114.123885

expression in presumptive stem cells to maintain the undifferentiated meristematic state (Byrne et al., 2000). Furthermore, ARP proteins act in the leaf to restrict KNOXI, such as BP, to the SAM. The mutually exclusive expression domains of *ARP* and *KNOXI* distinguishes leaf founder cell from meristem cell fate in the SAM (Long et al., 1996; Hay and Tsiantis, 2006). By contrast, some compound-leafed species, such as tomato (*Solanum lycopersicum*) and *Cardamine hirsuta*, show a reactivation of *KNOXI* expression during leaf development. An overlap of the expression domains of *ARP* and *KNOXI* was observed in these species (Hareven et al., 1996; Bharathan et al., 2002; Hay and Tsiantis, 2006; Champagne et al., 2007; Shani et al., 2009). However, expression analysis of *ARP* and *KNOXI* in pea (*Pisum sativum*), a compound-leafed legume belonging to the large inverted repeat-lacking clade (IRLC), shows they are expressed in complementary domains, like simple-leafed species and unlike tomato (Tattersall et al., 2005).

The lack of *KNOXI* expression in leaf primordia of the IRLC group indicates that *KNOXI* genes may not be involved in compound leaf formation in these legumes (Hofer et al., 2001; Champagne et al., 2007). Further studies demonstrate that the *FLORICAULA/LEAFY* (*LFY*) putative orthologs, pea *UNIFOLIATA* (*UNI*) and *Medicago truncatula SINGLE LEAFLET1* (*SGL1*) function in place of *KNOXI* to regulate compound leaf development (Hofer et al., 1997; Wojciechowski et al., 2004; Champagne et al., 2007; Wang et al., 2008). These findings raise questions on whether the *ARP-KNOXI* regulatory circuitry is still conserved in IRLC since the developmental process of the compound leaf has shifted away from the KNOXI-mediated module and how the *LFY* orthologs take over roles in compound leaf patterning in IRLC. However, the lack of *KNOXI* and *ARP* loss-of-function mutants in legumes hindered understanding of this distinct genetic regulation mechanism in compound leaf formation. Here, we address these questions by characterizing the *Tnt1* retrotransposon-tagged *ARP* and *STM/BP-like KNOXI* mutants in the model legume *M. truncatula*. We show that *M. truncatula ARP* (*PHAN*) and *STM/BP-like KNOXI* genes exhibit conserved functions. However, no genetic interactions between *PHAN* and *STM/BP-like KNOXI* genes were observed, suggesting that *STM/BP-like KNOXI* genes are uncoupled from *PHAN*. Furthermore, different responses to ectopic expression of *KNOXI* and *SGL1* reveal that *KNOXI* and *SGL1* regulate parallel pathways in leaf development, and *SGL1* probably functions in a stage-specific manner in regulating the indeterminate state of developing leaves in *M. truncatula*. Comparison of these developmental effects also sheds light on possible roles of other regulators in compound leaf patterning.

RESULTS

Identification of a *M. truncatula* Mutant with Defects in Leaf Development

To identify additional regulators that control leaf development, a *M. truncatula* mutant population (~13,000 independent lines) generated by tobacco (*Nicotiana tabacum*) *Tnt1* retrotransposon insertional mutagenesis (Tadege et al., 2008) was screened. One mutant line, NF2810, with obvious changes in leaf morphology was identified. Compared with the wild type, the mutant plant displayed downward-curled leaves with pronounced serrations on the leaf margin and needle-like stipules (Figures 1A to 1D) and occasionally produced leaves with ectopic leaflets and asymmetric lateral leaflets (Supplemental Figures 1A and 1B). In addition, mutant leaves exhibited elongated serrated tips at the margin area (Supplemental Figures 1C and 1D). At the reproductive stage, the petiole length in the mutant was significantly decreased, suggesting a compression of the leaf proximal-distal axis (Figures 1C and 1E). However, the length of rachis in the mutant did not show significant change (Figure 1F). Scanning electron microscopy analysis showed that the length of petiole epidermal cells in the mutant was drastically reduced compared with that in the wild type, suggesting that the reduced cell length accounted for the shortened petiole in the mutant (Figures 1G and 1H). The length of rachis epidermal cells was indistinguishable between the mutant and the wild type, but the cells in the mutant appeared thinner (Figures 1I and 1J). In addition, leaf epidermal cells were examined, and no obvious difference was observed between the mutant and wild type (Supplemental Figures 1E to 1H). Anatomical analysis revealed that 30% of midveins of the mutant leaf displayed ectopic vascular bundles (n = 10). Moreover, the phloem was enlarged on the abaxial side of the leaf of the mutant compared with that in the wild type (Figures 1K and 1L). Expanded phloem was also observed in the petiole of the mutant, suggesting that mutant leaves were partially abaxialized (Supplemental Figures 1I and1J).

YABBY and *HD-ZIP III* gene families are implicated in the establishment of abaxial and adaxial domains, respectively (Moon and Hake, 2011; Townsley and Sinha, 2012). To further evaluate the defects in leaf polarity of the mutant, the expression levels of *YABBY* and *HD-ZIP III* genes were analyzed (Supplemental Figure 2 and Supplemental Data Sets 1 and 2). Transcript levels of *HD-ZIP III* gene members varied between the wild type and mutant, but most *YABBY* genes were upregulated in the mutant, supporting the observation of abaxialized leaves in the mutant. In addition to the defects in leaf morphology, flower development in the mutant was also affected (Supplemental Figures 3A to 3J). The width of floral organs, such as the vexillum, was reduced in the mutant (Supplemental Figure 3K). The flowers were able to develop into seedpods, but the number of pods produced in the mutant was fewer than the wild type (Supplemental Figure 3L).

The Mutant Phenotype Is Associated With an *ARP* Ortholog in *M. truncatula*

To identify the gene associated with the mutant phenotype, thermal asymmetric interlaced-PCR was performed to recover the flanking sequences of *Tnt1* retrotransposon from the mutant. Based on PCR genotyping results, one flanking sequence segregating with the mutant phenotype was identified. A full-length genomic sequence was obtained using this flanking sequence to search against the *M. truncatula* genomic sequences in the National Center for Biotechnology Information database. The full-length coding sequence of 1080 nucleotides was obtained by RT-PCR. Alignment between the coding sequence (CDS) and the genomic sequence revealed that one intron is located at 5′ untranslated region of the gene (Figure 2A). Genomic PCR analysis was performed to detect the insertion site of the *Tnt1* retrotransposon. While an ~1.1-kb PCR fragment was amplified in the wild type, an ~6.4-kb PCR fragment

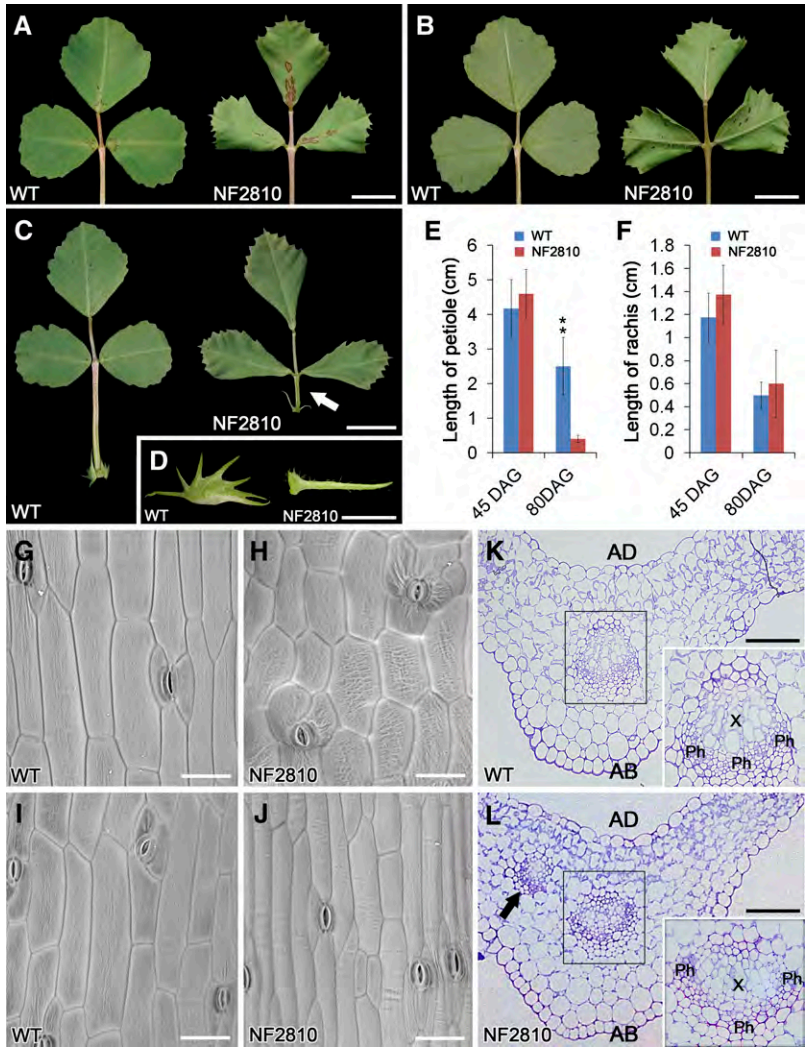

Figure 1. Defects in Leaf Development in the Mutant Plant.

(A) and **(B)** The adaxial side **(A)** and abaxial side **(B)** of fully expanded leaves from 45-d-old wild-type and mutant (NF2810) plants at vegetative stage.
(C) Fully expanded leaves from 80-d-old wild-type and mutant (NF2810) plants at reproductive stage. Arrow indicates shortened petiole of the mutant.
(D) Stipules of the wild type and the mutant.
(E) and **(F)** Lengths of petiole **(E)** and rachis **(F)** of the wild type and the mutant at different developmental stages. DAG, days after germination. Numbers are presented as means ± SD (n = 10). **P < 0.01.
(G) to **(J)** Scanning electron microscope images of epidermal cells of petiole (**[G]** and **[H]**) and rachis (**[I]** and **[J]**) from 80-d-old wild-type and mutant plants.
(K) and **(L)** Transverse sections of vascular bundles in leaf midveins of the wild type **(K)** and the mutant **(L)**. Arrow indicates ectopic vascular bundle. The insets in **(K)** and **(L)** show a close view of vascular bundles (boxed regions). Ph, phloem; X, xylem; AD, adaxial side; AB, abaxial side.
Bars = 1 cm in **(A)** to **(C)**, 5 mm in **(D)**, 50 μm in **(G)** to **(J)**, and 200 μm in **(K)** and **(L)**.
[See online article for color version of this figure.]

containing a single *Tnt1* retrotransposon (~5.3 kb) was amplified in the mutant (Figure 2B). Sequence comparison revealed that the *Tnt1* retrotransposon was inserted into the 3′ end of the second exon of this gene (Figure 2A; Supplemental Table 1). RT-PCR analysis showed that the full-length transcripts were interrupted in the mutant (Figure 2C). Quantitative RT-PCR (qRT-PCR) analysis was performed to measure gene expression levels using primers designed to amplify fragments upstream and downstream of the *Tnt1* insertion site. The results showed that transcript levels of this gene were very low (<9%) in the mutant, compared with that in the wild type (Supplemental Figure 4). Phylogenetic analysis revealed that this gene is a member of the MYB-domain protein family and evolutionarily closer to the pea *ARP* gene *CRISPA* (*CRI*), which is the ortholog of *A. majus PHAN* (Figure 2D; Supplemental Data Set 3) (Waites et al., 1998). BLAST analysis was performed against the *M. truncatula* genome sequence database (version Mt4.0V1,

www.jcvi.org/medicago/), and only one copy of this gene was found. Amino acid sequence comparison revealed high sequence similarity between this protein and ARP proteins from other plant species (Supplemental Figure 5). Based on these data, this gene is identified as the putative *ARP* ortholog in *M. truncatula* and named *PHAN*. A *Tnt1*-tagged mutant of *PHAN* was recently reported (Ge et al., 2014). Because the *Tnt1* insertion is located in the same position in the PHAN protein sequences of the mutants, the *PHAN* allele (Ge et al., 2014) is identical to the one in this study.

To further confirm that the *Tnt1* insertion in *PHAN* is responsible for the mutant phenotype, PCR reverse genetic screening of DNA pools from the *Tnt1*-tagged mutant population was performed (Tadege et al., 2008), but it failed to uncover additional alleles of *phan* from ~18,000 mutant lines. To rule out the possibility that the phenotype of *phan* is caused by other unknown mutations, *PHAN* knockdown plants were generated using RNA interference ($PHAN_{RNAi}$). The expression level of *PHAN* was dramatically reduced in the $PHAN_{RNAi}$ transgenic plants (Figure 2C). The leaf phenotype of the transgenic plants resembled that of *phan* (Figure 2E). Furthermore, a genomic fragment including the promoter and coding sequencing of *PHAN* was stably introduced into *phan* plants. The *phan* mutant phenotype was fully complemented (Figures 2F and 2G). Collectively, these data confirm that loss of function of *PHAN* resulted in developmental defects in the mutant. Expression pattern analysis based on the *M. truncatula* Gene Expression Atlas revealed relatively high levels of *PHAN* in vegetative buds, seeds, and pods (Supplemental Figure 6A). To determine the expression pattern more comprehensively, a *PHAN* promoter-GUS (β-glucuronidase) reporter gene was constructed and introduced into wild-type plants. GUS expression was detected in almost all organs (Supplemental Figures 6B to 6J), indicating broad roles of *PHAN* in the development of *M. truncatula*.

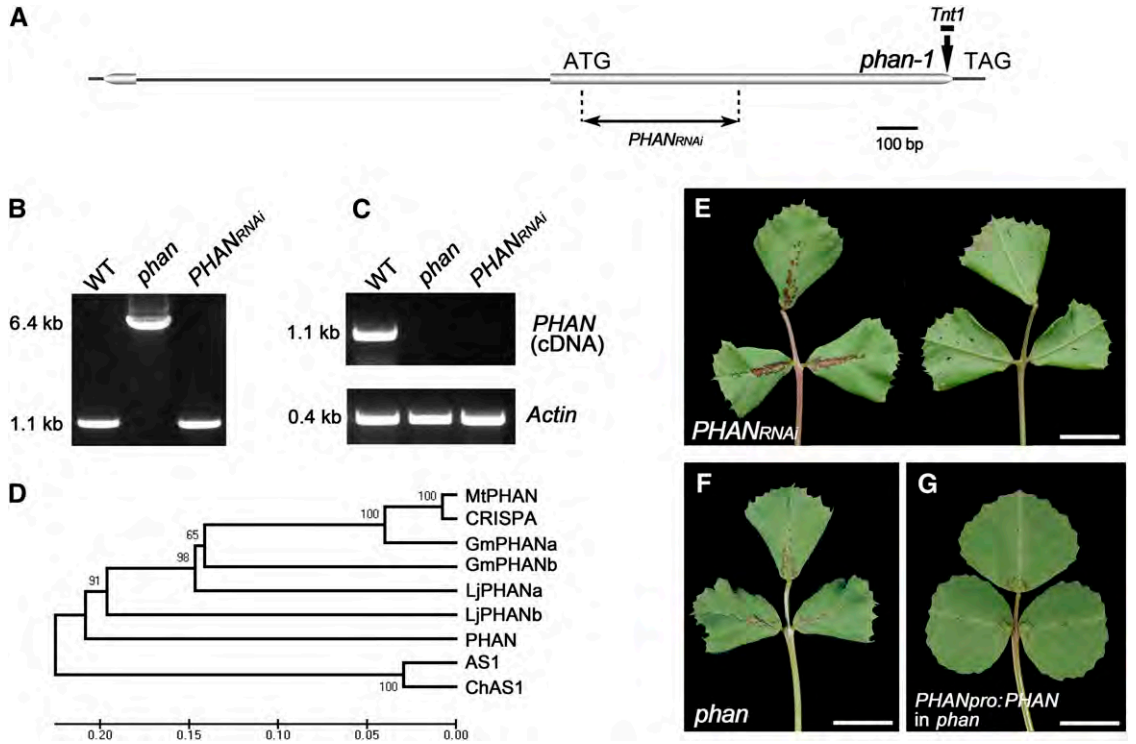

Figure 2. Molecular Cloning of *PHAN* in *M. truncatula*.

(A) *PHAN* gene structure and *Tnt1* insertion site. Boxes represent exons and lines represent intron. Vertical arrow marks the location of *Tnt1* retrotransposon in the *phan* mutant. Horizontal arrows mark the gene fragment used for the construction of the $PHAN_{RNAi}$ transgene.

(B) PCR identification of the *phan* mutant. An ~6.4-kb PCR fragment containing a single *Tnt1* retrotransposon (~5.3 kb) was amplified in the mutant. Wild-type and $PHAN_{RNAi}$ transgenic plants were used as controls.

(C) RT-PCR analysis of full-length transcripts of *PHAN* transcripts in vegetative buds of the *phan* mutant and $PHAN_{RNAi}$ transgenic plants. *ACTIN* was used as control.

(D) Phylogenetic analysis of *PHAN* and *ARP* genes from other species. Alignments used to generate the phylogeny are presented in Supplemental Data Set 3.

(E) Leaves of $PHAN_{RNAi}$ transgenic plants mimic the phenotype of *phan*.

(F) and **(G)** Genetic complementation of *phan*. Representative leaves of *phan* and *phan* transformed with the *PHANpro:PHAN* construct are shown in **(F)** and **(G)**, respectively.

Bars = 1 cm in **(E)** to **(G)**.

[See online article for color version of this figure.]

It has been shown that overexpression of *AS1* in *Arabidopsis* generated elongated and downwardly curling leaves (Theodoris et al., 2003), and overexpression of SlI-*PHAN* in tomato and tobacco produced ectopic blade outgrowth (Zoulias et al., 2012). To investigate the effects of ectopic *PHAN* expression, a cauliflower mosaic virus (CaMV) 35S promoter-driven *PHAN* transgene was introduced into the wild type. The transgenic plants did not display any obvious change in leaf morphology, suggesting that increased *ARP* activity results in different developmental responses among species (Supplemental Figures 6K and 6L).

STM/*BP-Like KNOXI* Activity Is Sufficient for Increasing Leaf Complexity

In a previous report, three class I (*KNOXI*) and three class II (*KNOXII*) *KNOX* genes were isolated in *M. truncatula* (Di Giacomo et al., 2008). By BLAST searching the *M. truncatula* genome sequence database (version Mt4.0V1, www.jcvi.org/medicago/), two additional *KNOXI* genes and two additional *KNOXII* genes were found. Phylogenetic analysis revealed that *KNOX1* and *KNOX6* were *STM-like* class I genes; *KNOX2* was a *BP-like* class I gene; and *KNOX7* and *KNOX8* were *KNAT2/6-like* class I genes (Supplemental Figure 7). In addition, Expression Atlas analysis showed that *KNOX1*, *2*, and *6* genes displayed similar expression patterns, and the patterns are different from that of *KNOX7* and *KNOX8* (Supplemental Figure 8). To start with, we focused on *KNOX1*, *KNOX2*, and *KNOX6* because the conserved regulatory module was reported mainly between *STM/BP-like KNOXI* genes and *ARP* (Kim et al., 2003b; Luo et al., 2005; Tattersall et al., 2005; Hay and Tsiantis, 2006). Previous studies showed that ectopic expression of *KNOXI* genes in compound-leafed species results in a dramatic increase in leaf complexity through promoting CK biosynthesis (Hareven et al., 1996; Jasinski et al., 2005; Yanai et al., 2005; Hay and Tsiantis, 2006; Champagne et al., 2007). To investigate whether *KNOXI* genes play such roles in *M. truncatula*, *KNOX1*, *KNOX2*, and *KNOX6*, under control of the constitutive CaMV 35S promoter, were introduced into the wild type. One of the *KNOXII* genes, *KNOX4*, was also overexpressed as a control. Transgenic plants (*OX-KNOXI*) with increased expression levels of *STM/BP-like KNOXI* genes exhibited a similar reiteration of higher order leaflets along elongated petiolules, and variations in leaflet number and shape were also observed (Figures 3A to 3F). These observations demonstrate that the ectopic *STM/BP-like KNOXI* activity is sufficient for increasing leaf complexity in *M. truncatula*. The transgenic plants overexpressing *KNOX4* did not show obvious changes in leaf morphology, suggesting distinct functional roles between *KNOXI* and *KNOXII* genes (Figure 3G).

STM/*BP-Like KNOXI* Genes Are Not under Negative Control of *PHAN*

To assess if *PHAN* has conserved function, the *PHAN* coding sequence under control of the CaMV 35S promoter was introduced into the *Arabidopsis as1* mutant. The mutant phenotype was fully complemented, and the ectopic expression of *BP* in *as1* was repressed in the transgenic plants, indicating functional equivalence between *M. truncatula PHAN* and *Arabidopsis AS1* (Figures 4A to 4D). Previous studies showed that *ARP* is a negative regulator of *KNOXI* genes (Tsiantis et al., 1999; Kim et al., 2003b; Tattersall et al., 2005; Hay and Tsiantis, 2006; Guo et al., 2008). To investigate whether *PHAN* plays a conserved role to repress the *STM/BP-like KNOXI* genes in leaves of *M. truncatula*, the expression levels and domains of *KNOX1*, *2*, and *6* genes were analyzed. qRT-PCR data showed that the expression levels of *KNOX1*, *2*, and *6* genes remained unchanged in both leaf and petiole in the *phan* mutant, compared with that in the wild type (Figures 4E and 4F). The spatial localization of *KNOX1*, *2*, and *6* in the wild type and the *phan* mutant was further compared by RNA in situ hybridization analysis. In the wild type, the expression of *KNOX1*, *2*, and *6* genes was detected in the SAM but excluded from incipient leaf primordia (P0) and developing leaf primordia (Figures 4G, 4I, and 4K). In the *phan* mutant, expression patterns of three *KNOXI* genes were essentially the same as those in the wild type (Figures 4H, 4J, and 4L), indicating that loss of *PHAN* did not lead to ectopic expression of the *STM/BP-like KNOXI* genes.

Simultaneous Disruption of *STM*/*BP-Like KNOXI* Genes Cannot Rescue the *phan* Phenotype

To better understand the functions of *STM/BP-like KNOXI* genes, a PCR reverse genetic screening of the *Tnt1*-tagged mutant population was performed to isolate relevant loss-of-function mutants. Two, two, and three independent mutant lines were identified for *KNOX1*, *KNOX2*, and *KNOX6*, respectively. The *Tnt1* retrotransposon was detected in the exons of these genes (Figures 5A to 5C; Supplemental Table 1). RT-PCR analysis showed that full-length transcripts of the three genes were abolished in respective homozygous mutant plants (Figure 5D). Transcript levels of *KNOX1*, *2*, and *6* genes in the mutant alleles were further measured by qRT-PCR using primer pairs designed to amplify fragments upstream and downstream of the *Tnt1* insertion sites (Supplemental Figure 9). The results revealed that the expression levels of *KNOX1*, *2*, and *6* were extremely low (<5%) in the mutants.

Loss of function in *KNOX1*, *KNOX2*, or *KNOX6* did not lead to obvious defects in SAM maintenance and leaf morphology (Figure 5E). To assess functional redundancy among *STM/BP-like KNOXI* genes, double mutants and triple mutants were generated. No obvious developmental changes were observed in double mutants derived from different cross combinations among *knox1*, *knox2*, and *knox6*. Simultaneous disruption of three *KNOXI* genes resulted in semidwarf plants (Supplemental Figures 10A and 10B), suggesting that *STM/BP-like KNOXI* genes are required for plant vegetative growth. The leaves in the triple mutant were normal, indicating that *STM/BP-like KNOXI* genes are not involved in compound leaf patterning in *M. truncatula* (Figure 5E).

To further investigate potential genetic interactions between *PHAN* and *STM/BP-like KNOXI* genes, double, triple, and quadruple mutants were generated among the relevant mutants. Knockout of any or all *KNOX1*, *2*, and *6* genes in the *phan* background did not rescue leaf defects, such as downward-curled leaves (Figure 5F) and shortened petioles (Supplemental Figures 10C and 10D). These genetic evidences in combination with the expression pattern analysis (Figures 4G to 4L) demonstrate that *PHAN* does not negatively regulate the expression of *STM/BP-like KNOXI* genes in *M. truncatula*.

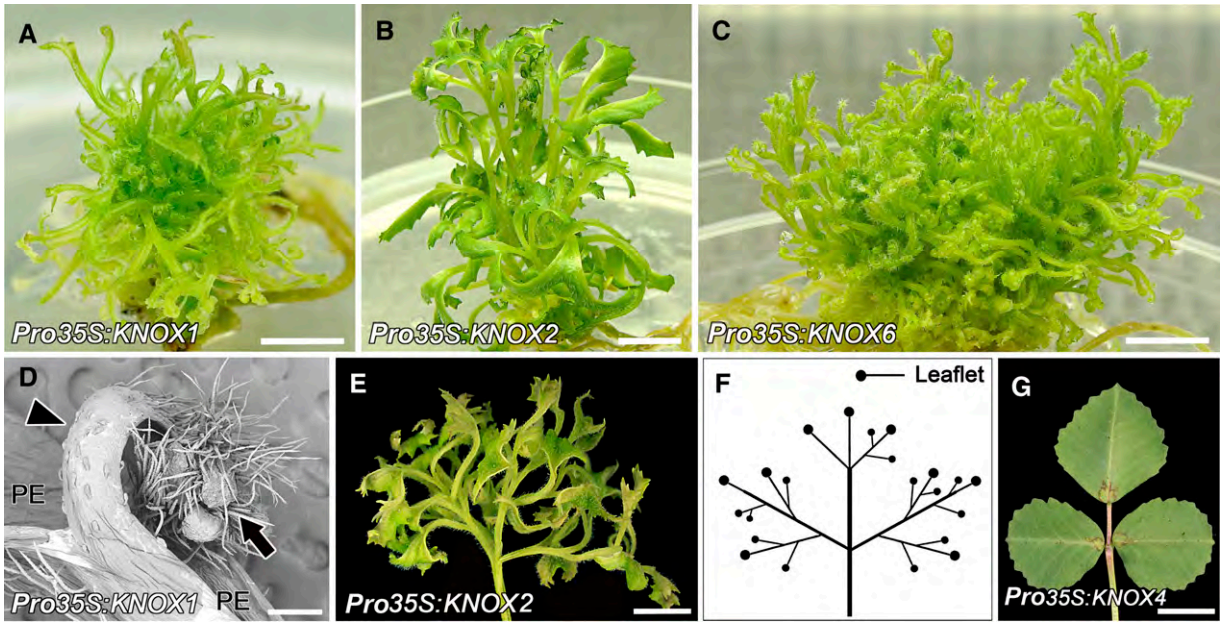

Figure 3. Functional Analysis of *KNOXI* Genes in *M. truncatula*.

(A) to **(C)** Transgenic plants overexpressing *Pro35S:KNOX1*, *Pro35S:KNOX2*, and *Pro35S:KNOX6*.
(D) Scanning electron microscope image shows a representative leaf derived from the *Pro35S:KNOX1* transgenic plants. The ectopic leaflet (arrowhead) is developing along the petiolule and higher order leaflets are developing (arrow). PE, petiolule.
(E) and **(F)** A representative leaf derived from a *Pro35S:KNOX2* transgenic plant **(E)** and its schematic illustration **(F)**. A dramatic increase in leaf complexity is shown.
(G) A representative leaf derived from a *Pro35S:KNOX4* transgenic plant.
Bars = 1 cm in **(A)** to **(C)**, **(E)**, and **(G)** and 200 μm in **(D)**.
[See online article for color version of this figure.]

STM/BP-Like KNOXI Genes Do Not Repress *PHAN*

In *Arabidopsis*, *STM* represses *AS1* expression in the meristem, and the *as1* mutant can partially rescue the *stm* phenotype (Byrne et al., 2000; Hay et al., 2006). To investigate the possible suppression of *STM/BP-like KNOXI* genes on *PHAN*, the spatial and temporal localizations of *PHAN* were examined by RNA in situ hybridization in the wild type and *knox1*, *2*, and *6* mutants. In the wild type, *PHAN* mRNA was detected throughout the whole SAM and in both adaxial and abaxial sides of developing leaf primordia (Figures 6A and 6B). Transverse sections through developing leaflets showed that *PHAN* expression was more localized in the leaflet in the P6 primordium (Figure 6C). In the older P7 primodium, *PHAN* transcripts were confined to the adaxial side of the medial portion of leaf lamina (Figure 6D). Such adaxial expression of *PHAN* was also detected in the rachis and petiole at this developmental stage (Figure 6E). The *PHAN* expression pattern was further assessed in the *knox1*, *2*, and *6* mutant backgrounds. RNA in situ hybridization revealed that expression patterns of *PHAN* in SAM of the single/double/triple *knox1*, *2*, and *6* mutants (Figures 6G to 6I and 6K) were similar to that of the wild type (Figures 6A and 6B). The expression domain of *PHAN* was also adaxialized in developing leaf lamina of the *knoxi* mutants (Figures 6J and 6L), similar to the wild type (Figure 6D). qRT-PCR data further confirmed that the expression levels of *PHAN* were unchanged in vegetative buds and other plant tissues between the wild type and the *knox1*, *2*, and *6* mutants (Supplemental Figure 11). These observations suggest that *STM/BP-like KNOXI* genes do not suppress the expression of *PHAN* in *M. truncatula*.

Compromising Auxin Transportation Mediated by *SLM1* Does Not Affect *STM/BP-Like KNOXI* Gene Expression

It has been shown that proper auxin transport regulated by *PIN-FORMED1* (*PIN1*) and *AS1* converge to repress *BP* expression in *Arabidopsis*, and the defects of the *pin1* mutant are partially rescued in the *pin1 bp* double mutant (Hay et al., 2006). A *PIN1* ortholog, *SMOOTH LEAF MARGIN1* (*SLM1*), has been identified in *M. truncatula* (Zhou et al., 2011). Auxin distribution is impaired in the *slm1* mutant, indicating conserved roles of *SLM1* in auxin transportation. To determine whether the auxin/SLM1 module is a possible repressor of *STM/BP-like KNOXI* in *M. truncatula*, the expression levels of *KNOXI* genes were analyzed in the *slm1* mutant (Figure 7A). The transcript levels of *KNOX1*, *2*, and *6* genes remained essentially unchanged in *slm1*, indicating that *SLM1* is not involved in the repression of *KNOXI* genes. To further test whether spatial and temporal expression of *STM/BP-like KNOXI* genes contributed to the defects of *slm1*, double, triple, and quadruple mutants among *slm1* and *knoxi* mutants were generated (Figure 7B). The phenotype of the *slm1-1 knox2-1* double mutant is similar to that of *slm1-1*. On the other hand, the *slm1-1 knox1-1 knox6-1* triple mutant is semidwarf, displaying fewer clustered leaves and shortened stems. Leaflet initiation was severely reduced when all three *KNOXI* genes were

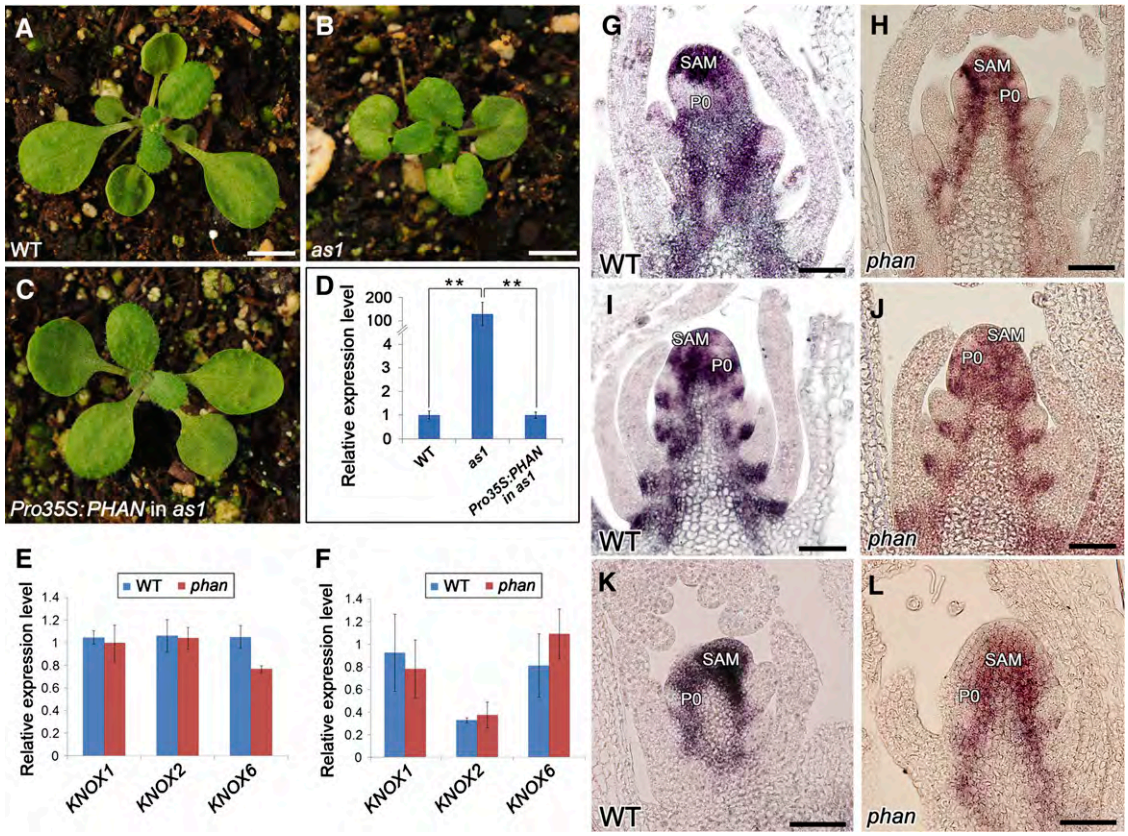

Figure 4. Functional Analysis of *PHAN* in *Arabidopsis* and *M. truncatula*.

(A) to **(D)** Genetic complementation of the *Arabidopsis as1* mutant. Transcript levels were measured by qRT-PCR. Values are the means and SD of three biological replicates. **P < 0.01.

(A) Rosettes of *Arabidopsis* wild type.

(B) *as1* mutant.

(C) *Pro35S:PHAN* in *as1* mutant.

(D) Expression levels of *BP* in leaves of the wild type, *as1*, and *Pro35S:PHAN* in *as1* background.

(E) and **(F)** Transcript levels of the *KNOXI* genes in leaf blade **(E)** and petiole **(F)** of the wild type and *phan*. Transcript levels were measured by qRT-PCR. Values are the means and SD of three biological replicates.

(G) to **(L)** Expression patterns of *KNOX1* (**[G]** and **[H]**), *KNOX2* (**[I]** and **[J]**), and *KNOX6* (**[K]** and **[L]**) in the wild type and *phan*. Longitudinal sections of SAM are shown. P0, incipient leaf primordia.

Bars = 5 mm in **(A)** to **(C)** and 50 μm in **(G)** to **(L)**.

[See online article for color version of this figure.]

simultaneously disrupted in *slm1-1*. These observations suggest that *SLM1* and *STM/BP-like KNOXI* genes probably function redundantly in leaf initiation. However, the defects in floral development and seed production in *slm1* could not even be partially rescued by introducing various *knoxi* mutations (Figure 7C). This result suggests that the *slm1* mutant phenotype could not be attributed to the *STM/BP-like KNOXI* genes in *M. truncatula*, which is distinctly different from that in *Arabidopsis*. To further test whether *PHAN* and *SLM1* converge to repress *KNOXI* expression, the *phan slm1* double mutant was generated. Leaves of the *phan slm1* double mutant showed an additive phenotype (Figure 7D). The expression levels of *KNOX1*, *2*, and *6* genes did not change in the *phan slm1* double mutant (Figure 7E), further confirming that *STM/BP-like KNOXI* genes are not under the negative regulation of either *SLM1* or *PHAN*.

Ectopic Expression of *SGL1* Fails to Increase Leaf Complexity but Mimics *phan* Phenotype

As previously suggested, the *LFY* putative ortholog, *SGL1*, functions in place of *KNOXI* genes to regulate compound leaf development (Champagne et al., 2007; Wang et al., 2008). To determinate whether increased *SGL1* activity is sufficient to increase leaf complexity, *SGL1* was overexpressed under control of the CaMV 35S promoter. Overexpression of *SGL1* (*OX-SGL1*) did not produce extra leaflets on rachis in transgenic plants (Figure 8A), indicating that increased *SGL1* activity does not alter the indeterminacy of developing leaves. It was observed that the leaves of *OX-SGL1* plants displayed a downward-curled leaf margin and elongated stipule (Figures 8A and 8B), which partially mimic the phenotype of *phan* (Figures 1A and 1D). This

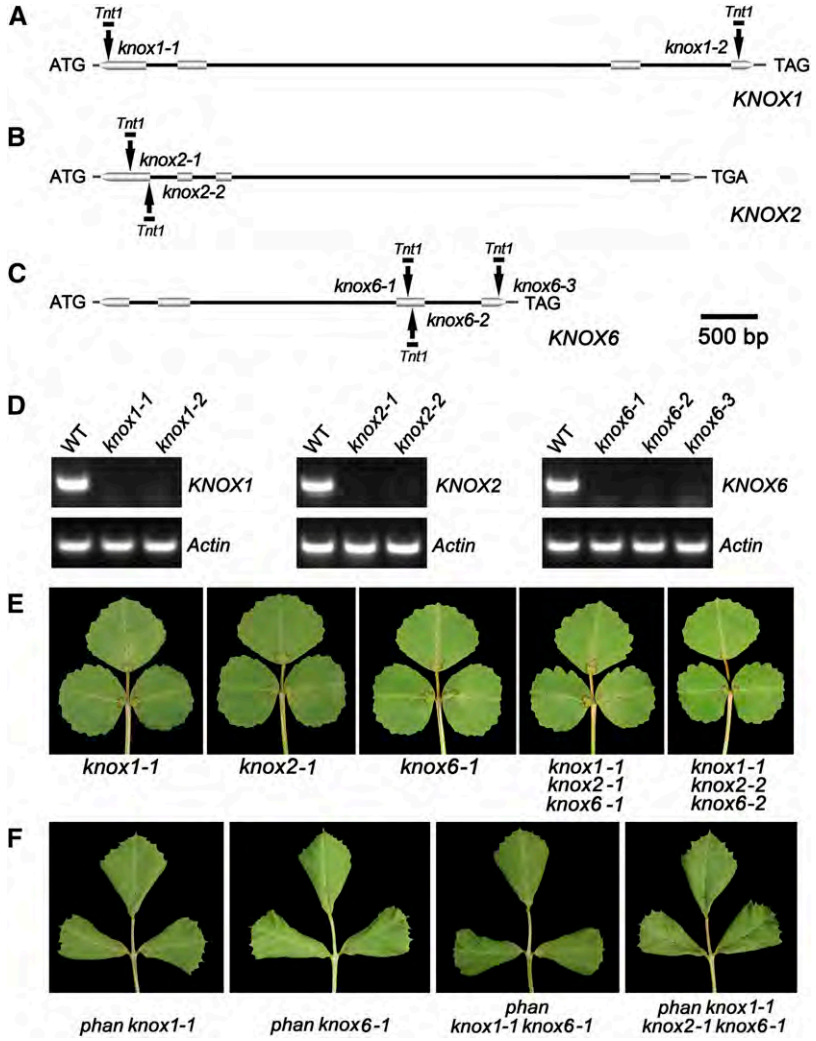

Figure 5. Characterization of Loss-of-Function Mutants of *STM/BP-Like KNOXI* Genes.

(A) to **(C)** Schematic representations of gene structures of *KNOX1* **(A)**, *KNOX2* **(B)**, and *KNOX6* **(C)**. Boxes represent exons and lines represent introns. Vertical arrows mark the location of *Tnt1* retrotransposon in different mutant alleles.

(D) RT-PCR analysis of full-length transcripts of *KNOX1*, *KNOX2*, and *KNOX6* in vegetative buds of wild-type and different mutant alleles. *ACTIN* was used as control. Three biological replicates were performed.

(E) Representative leaves of *knox1*, *knox2*, and *knox6* single mutants and *knox1 knox2 knox6* triple mutants.

(F) Representative leaves of double, triple, and quadruple mutants of the *phan* and *knoxi* mutants. No obvious difference was observed among them. [See online article for color version of this figure.]

observation suggests two possibilities: *SGL1* represses *PHAN* expression in *OX-SGL1* transgenic plants, or *SGL1* expression is up-regulated in the *phan* mutant. However, qRT-PCR results showed that transcript levels of *PHAN* (Figure 8C) and *SGL1* (Figure 8D) were not altered in *OX-SGL1* or *phan*, indicating no direct interaction between them at the transcriptional level. To further investigate the genetic interaction between *PHAN* and *SGL1*, the *sgl1 phan* double mutant was generated (Figures 8E to 8H; Supplemental Figure 12). The double mutant showed additive defects in leaf phenotype by displaying downward-curled simple leaves. Furthermore, *sgl1 phan* developed a significantly shorter petiole than the *sgl1* or *phan* single mutant (Figure 8I), suggesting an additive interaction between *SGL1* and *PHAN* in the development of leaf proximal-distal axis.

The *KNAT2/6-Like* Class I Gene *KNOX7* Is Likely Repressed by *PHAN*

It has been shown that *AS1* represses the expression of *KNAT2* and *KNAT6*, in addition to *BP* in *Arabidopsis* (Byrne et al., 2000; Ori et al., 2000; Semiarti et al., 2001; Guo et al., 2008). To test if *KNAT2/6-like* Class I genes were negatively regulated by *PHAN* in *M. truncatula*, qRT-PCR was performed to analyze expression levels of *KNOX7*

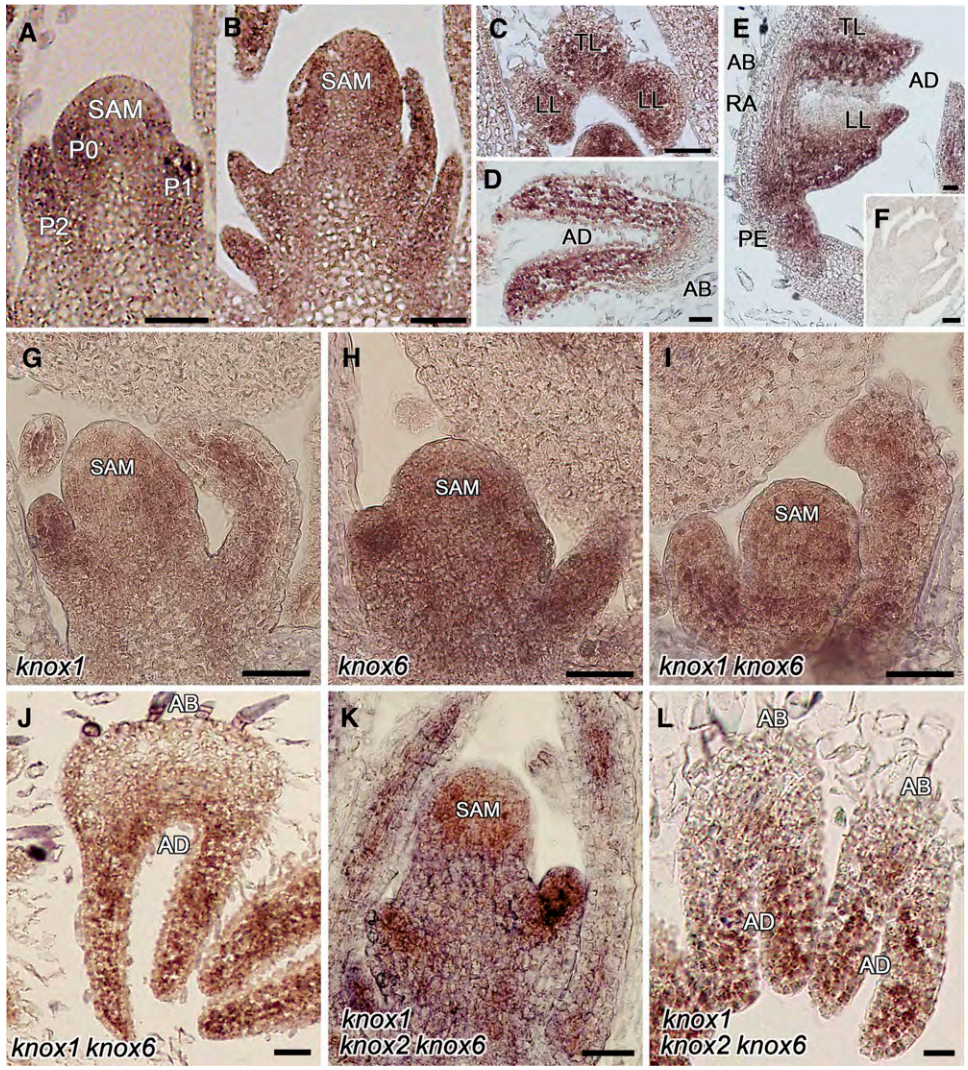

Figure 6. Expression Patterns of *PHAN* in the Wild Type and *knox1*, *2*, and *6* Mutants.

(A) to **(F)** RNA in situ hybridization analysis of *PHAN* mRNA in vegetative apices of the wild type. Longitudinal sections of shoot apical meristem and leaf primordia are shown in **(A)** and **(B)** at early developmental stages. Transverse sections of developing leaflets of P6 and P7 primordia are shown in **(C)** and **(D)**, respectively. Longitudinal section of a leaf in primordium P7 is shown in **(E)**. No expression was detected using a control sense *PHAN* probe **(F)**.
(G) to **(L)** Expression patterns of *PHAN* in *knox1-1* **(G)** and *knox6-1* **(H)** single mutants, *knox1-1 knox6-1* double mutants **(I)** and **(J)**, and *knox1-1 knox2-1 knox6-1* triple mutants **(K)** and **(L)**. Longitudinal sections of SAM are shown in **(G)** to **(I)** and **(K)**. Transverse sections of developing leaflets are shown in **(J)** and **(L)**. P, plastochron; AD, adaxial side; AB, abaxial side; PE, petiole; RA, rachis. Bars = 50 μm in **(A)** to **(L)**.
[See online article for color version of this figure.]

and *KNOX8* in different tissues. A significant increase in the level of *KNOX7* transcript was detected in the petiole of the *phan* mutant, while no change was found in the leaf blade (Figures 9A and 9B). No significant difference was detected in *KNOX8* expression in either leaf blade or petiole in *phan*, compared with the wild type (Figures 9A and 9B). The spatial localizations of *KNOX7* were examined by in situ hybridization analysis. The results showed that *KNOX7* was expressed in the SAM but excluded from incipient leaf primordia (P0) and developing leaf primordia in the wild type, which is similar to that of *KNOX1*, *2*, and *6* genes. In the *phan* mutant, however, ectopic expression of *KNOX7* was detected in the P0 primordia, and a signal was also detectable in the P1 primordia (Figures 9C to 9F). These data indicate that *KNOX7* may be under the negative regulation of *PHAN*. Future identification and characterization of loss-of-function *KNOX7* and *KNOX8* mutants are needed to provide more convincing evidence.

DISCUSSION

The Function of *ARP* Genes Is Species Specific

Loss of function of *PHAN* in *A. majus* resulted in abaxialized leaves (Waites et al., 1998). However, *Arabidopsis as1* and

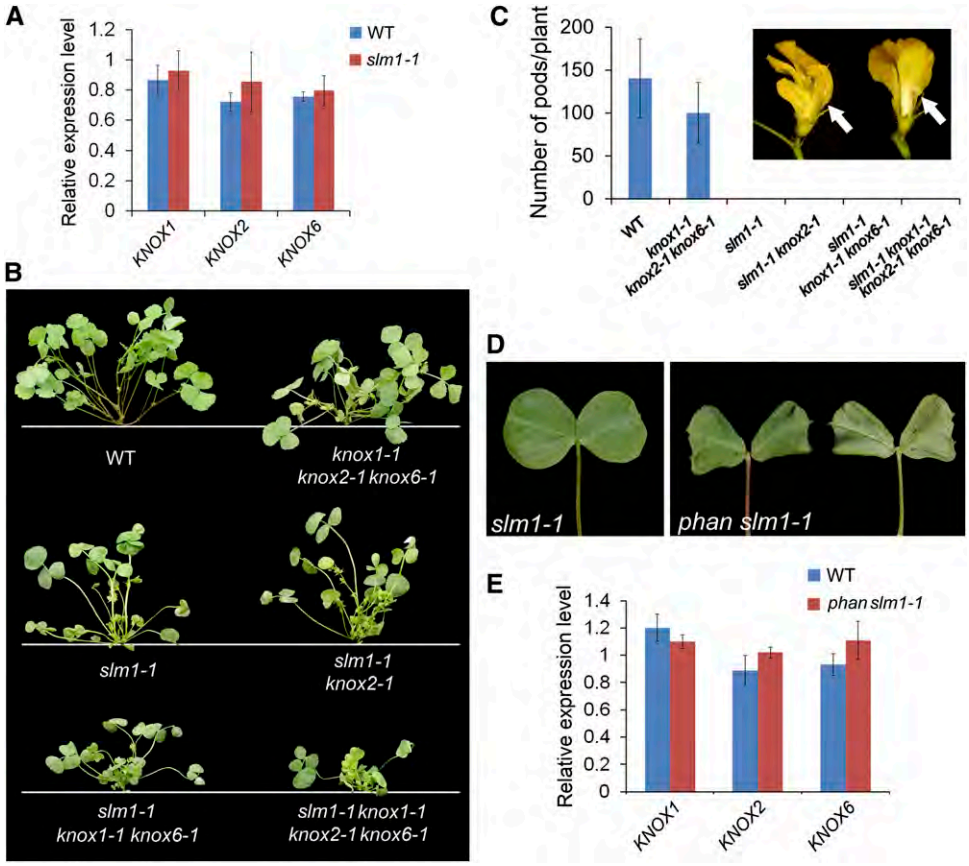

Figure 7. The Auxin/SLM1 Module Is Not a Repressor of *STM/BP-Like KNOXI* Genes.

(A) Expression levels of the *KNOXI* genes in vegetative buds of the wild type and *slm1-1*. Transcript levels were measured by qRT-PCR. Values are the means and SD of three biological replicates.
(B) Plants of the wild type and mutants derived from different cross combinations among *slm1-1* and *knoxi* mutants.
(C) Seedpod production in the wild type and mutants. The inset shows the flower phenotype of *slm1-1* (left) and *slm1-1 knox1-1 knox2-1knox6-1* quadruple mutant (right). Arrows point to the fused floral organs. Numbers are presented as means ± SD (n = 5).
(D) Leaves of *slm1-1* and *phan slm1-1* double mutant.
(E) Expression levels of *KNOXI* genes in vegetative buds of the wild type and *phan slm1-1* double mutant. Values are the means and SD of three biological replicates.
[See online article for color version of this figure.]

maize *rs2* mutants did not show obvious defects in leaf polarity (Schneeberger et al., 1998; Serrano-Cartagena et al., 1999). Moreover, in compound-leafed species, various leaf patterning was observed when *ARP* orthologs were suppressed. Down-regulation of *ARP* in tomato resulted in altered leaflet number and leaf shape (Kim et al., 2003a). A mutation in *AS1* in *C. hirsuta* led to increased leaflet number by developing extra leaflets (Hay and Tsiantis, 2006). The pea *cri* mutant developed abaxialized leaflets and ectopic stipules and had only minor effects on leaf complexity (Tattersall et al., 2005). In *M. truncatula*, the length of rachis in the *phan* mutant was similar to that of the wild type, although leaves with longer rachis were observed on some nodes in the *phan* mutant (Ge et al., 2014). The most obvious defects displayed in the *phan* mutant were narrow laminae and shortened petioles, which were similar to those in the *cri* mutant. It should be noted that the *Tnt1* insertion is located at the 3′ end of the *PHAN* coding sequence, and the 9% *PHAN* expression detected in the mutant could result in some residual function. Although both *M. truncatula* and pea are IRLC members, their leaf complexities are different. *M. truncatula* has the simplest compound leaf form consisting of only three leaflets with the same identity, while pea possesses a more complex leaf form including highly specialized tendrils. Even so, neither leaflet number nor leaf identity was altered in *phan* and *cri* mutants regardless of their leaf complexity. According to these observations, it appears that *PHAN* orthologs may play limited roles in the elaboration of compound leaves in IRLC species. Furthermore, increased *ARP* activities led to different phenotypic output among species. Overexpression of *AS1* in *Arabidopsis* or *PHAN* in *M. truncatula* did not alter leaf complexity, such as reiteration of lobes or leaflets (Theodoris et al., 2003). However, ectopic expression of *PHAN* in tomato produced an

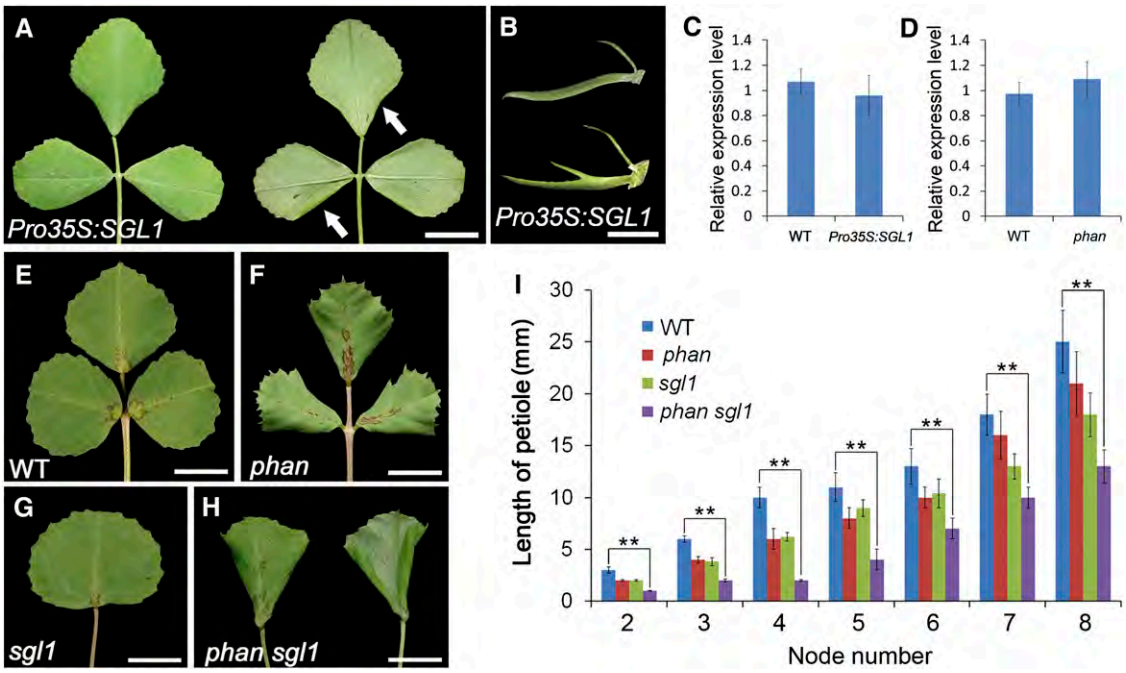

Figure 8. Functional Analysis of *SGL1* and Its Genetic Interactions with *PHAN*.

(A) and **(B)** Representative leaves **(A)** and stipules **(B)** derived from *OX-SGL1* transgenic plants. Adaxial and abaxial sides of the leaf are shown in **(A)**. Arrows point to the downward curved leaf margin.

(C) and **(D)** Expression levels of *PHAN* **(C)** and *SGL1* **(D)** in vegetative buds of *OX-SGL1* transgenic plants and the *phan* mutant, respectively. Transcript levels were measured by qRT-PCR. Values are the means and SD of three biological replicates.

(E) to **(H)** Leaf phenotype of wild type **(E)**, *phan* mutant **(F)**, *sgl1* mutant **(G)**, and *phan sgl1* double mutant **(H)**.

(I) Lengths of petiole at different nodes in 80-d-old wild-type and mutant plants. Numbers are presented as means ± SD (n = 10). **P < 0.01.

Bars = 1 cm in **(A)** and **(E)** to **(H)** and 5 mm in **(B)**.

ectopic adaxial domain in leaves, leading to defects in leaf patterning. Thus, these observations imply that *ARPs* function in a species-specific manner during leaf development. We performed a comparative analysis and summarized *ARP* expression patterns among species (Supplemental Figure 13).

Although pea is a member of IRLC and *Lotus japonicus* is not, the expression patterns of *CRI* and Lj-*PHANa/b* are similar. Their transcripts were detected at sites of leaf initiation (P0), but excluded from the SAM, forming a mutually exclusive pattern with *KNOXI* genes. To our surprise, *M. truncatula PHAN* has a distinct expression pattern, compared with those in *Arabidopsis*, *C. hirsute*, and other legume species (Byrne et al., 2000; Luo et al., 2005; Tattersall et al., 2005; Hay and Tsiantis, 2006) (Supplemental Figure 13). *M. truncatula PHAN* is diffusely expressed throughout the SAM, showing an overlapping expression domain with *KNOXI* genes. The diffused expression of *M. truncatula PHAN* in the SAM is similar to that in tomato and distinctly different from that in pea, even though *M. truncatula* and pea are evolutionarily close to each other. On the other hand, *ARP* expression domains are associated with the adaxial side of leaf primordia at early developmental stages in compound-leafed species. For example, *PHAN* displayed adaxial expression in the P3/P4 leaf primordia of tomato (Kim et al., 2003a, 2003b), P1 of *L. japonicus* (Luo et al., 2005), and P3 of pea (Tattersall et al., 2005) (Supplemental Figure 13). In *M. truncatula*, *PHAN* transcripts were detected in both the adaxial and abaxial sides of leaf primordia from P1 to P5. However, *PHAN* mRNA was confined to the adaxial side of the leaf at the late developmental stage (P6/P7). The adaxial expression of *PHAN* during leaf development implies that it may play a role in leaf polarity maintenance, as evidenced by the partially abaxialized leaf and upregulated *YABBY* expression in the *phan* mutant. Taken together, these results suggest that the roles of *ARP* orthologs vary with species, resulting in different developmental effects among species.

STM/BP-Like KNOXI Genes Are Uncoupled from *PHAN*

In *Arabidopsis*, *STM* represses *AS1* expression in the SAM, and the *as1* mutant can rescue the *stm* phenotype (Byrne et al., 2000). A similar regulatory relationship was also reported in tomato where Le-*T6* is a negative regulator of *PHAN* (Kim et al., 2003b). Moreover, *PHAN* negatively regulates *STM* in *A. majus* (Tsiantis et al., 1999) and *BP* orthologs in *Arabidopsis*, *C. hirsuta*, tomato, and pea (Kim et al., 2003b; Tattersall et al., 2005; Hay and Tsiantis, 2006; Guo et al., 2008). In this study, we investigated the relationship between *PHAN* and *STM/BP-like KNOXI* genes in *M. truncatula*. Unexpectedly, our results provide evidences that argue against the conserved relationship between *PHAN* and *STM/BP-like KNOXI* genes reported previously. First, the *PHAN* expression level and pattern did not change in single and multiple mutants of both *STM-like* and *BP-like KNOXI* genes. Similarly, the expression levels of *STM/BP-like KNOXI*

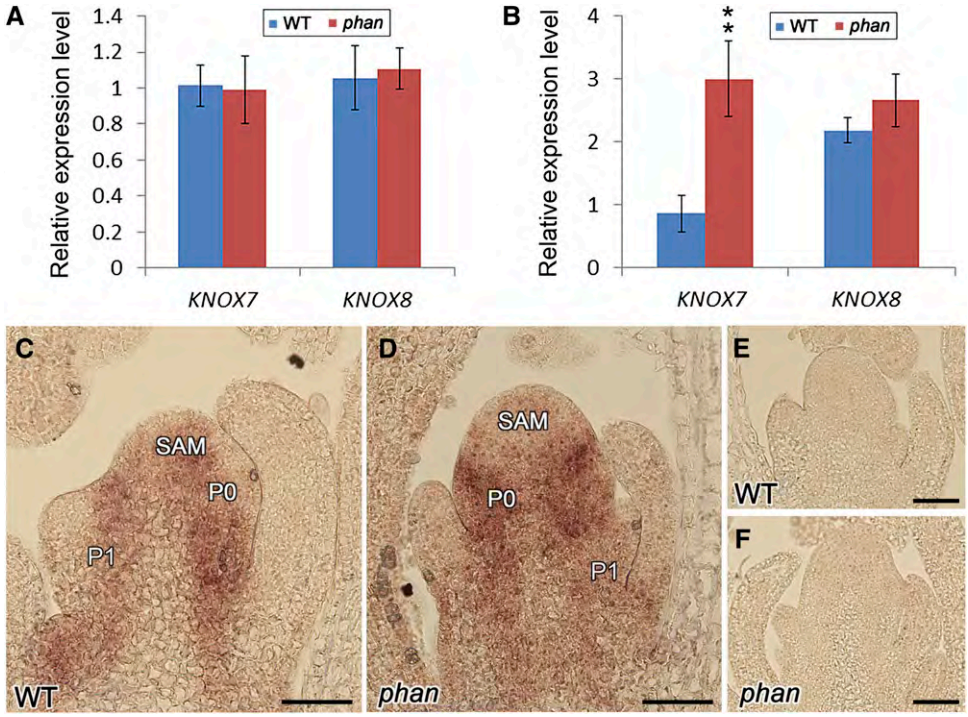

Figure 9. Expression of *KNAT2/6-like* Class I Gene *KNOX7* in the Wild Type and the *phan* Mutant.

(A) and **(B)** Transcript levels of the *KNOX7* and *KNOX8* in leaf blade **(A)** and petiole **(B)** of the wild type and the *phan* mutant. Transcript levels were measured by qRT-PCR. Values are the means and SD of three biological replicates. **P < 0.01.

(C) to **(F)** Expression patterns of *KNOX7* in the wild type **(C)** and *phan* **(D)**. Longitudinal sections of SAM are shown. No expression was detected using a control sense *KNOX7* probe (**[E]** and **[F]**). P, plastochron. Bars = 50 μm.

[See online article for color version of this figure.]

genes did not show significant changes in the *phan* mutant either. In another report, *STM/BP-like KNOXI* genes were upregulated slightly (<2-fold) in shoot buds of the *phan* mutant (Ge et al., 2014). However, such an increase of *KNOXI* expression in *phan* is not comparable with the upregulation of *BP* in *as1* (>100-fold) (Hay et al., 2006). Second, genetic evidence showed that knockout of *STM/BP-like KNOXI* genes failed to rescue the *phan* phenotype. These results together indicate that it is unlikely that the conserved regulatory circuitry between *PHAN* and *STM/BP-like KNOXI* genes exists in *M. truncatula*. Additionally, previous studies reported that *BP* expression is repressed by *PIN1*-mediated auxin transport in *Arabidopsis*. Loss of *BP* activity partially rescued the defects in the *pin1* mutant (Hay and Tsiantis, 2006). In *M. truncatula*, however, compromising *SLM1* activity did not lead to ectopic expression of the *BP-like KNOXI* gene. Furthermore, knockout of any or all *STM/BP-like KNOXI* genes failed to rescue the defects in flower development and seed production in the *slm1* mutant. Overall, our data support that *STM/BP-like KNOXI* genes are uncoupled from *PHAN*.

The suppression of growth along the proximal-distal axis was observed in *arp* mutants in several species, and the trait has been associated with ectopic expression of *KNOXI* genes (Tattersall et al., 2005; Hay et al., 2006; Hay and Tsiantis, 2006). In *Arabidopsis*, *KNAT2* and *KNAT6* are under the negative regulation of *AS1* (Byrne et al., 2000; Ori et al., 2000; Semiarti et al., 2001; Guo et al., 2008). Our data also showed that the *KNAT2/6-like* Class I gene *KNOX7* is upregulated in the petiole of the *phan* mutant, suggesting that ectopic expression of *KNOX7* may contribute to the *phan* phenotype. The expression of *KNOX8* remains essentially unchanged between the wild type and *phan*, indicating that *KNOX8* may not be associated with *PHAN*. The expression domain of *KNOX7* overlapped with that of *PHAN* in the SAM, although *KNOX7* was repressed in the incipient leaf primordia. Similar overlapping between *PHAN* and *TKN1* was observed in the SAM of tomato (Kim et al., 2003b). This observation implies that other genes may be involved in the repression of *KNOX7*, and the regulation mechanism of *KNOX7* is not universal in different developmental domains. It has been suggested that *KNOXI* genes play redundant roles in SAM maintenance in *Arabidopsis* (Byrne et al., 2002; Belles-Boix et al., 2006), rice (Tsuda et al., 2011), and maize (Bolduc et al., 2013). In this study, simultaneous disruption of three *STM/BP-like KNOXI* genes did not affect SAM function in *M. truncatula*. Therefore, future identification of loss-of-function mutants of *KNAT2/6-like KNOXI* genes will help clarify (1) whether *STM/BP-like KNOXI* genes and *KNAT2/6-like KNOXI* genes function redundantly in SAM maintenance; (2) whether *KNAT2/6-like KNOXI* genes are repressors of *PHAN*; and (3) how the developmental process of compound leaves in IRLC shifts away from the regulation mechanism mediated by the *KNOXI* gene family.

KNOXI and *LFY* Orthologs May Regulate Parallel Pathways in IRLC

Previous studies have found that *LFY* orthologs, instead of *KNOXI* genes, are essential for compound leaf development in IRLC species (Champagne et al., 2007). Loss of function of *LFY* orthologs in pea and *M. truncatula* resulted in the formation of simple leaves (Hofer et al., 2001; Wang et al., 2008). Moreover, leaf complexity was increased in pea *afila* mutants in which the *LFY/UNI* expression level was upregulated (Mishra et al., 2009). These observations imply that *LFY* activities are necessary and sufficient for regulating indeterminacy during leaf development. However, to date, there has been no direct evidence that increased activities of *LFY* orthologs could prolong the window of morphogenetic plasticity during leaf development in IRLC species. In this study, comparative analysis of *OX-KNOXI* and *OX-SGL1* transgenic plants shed light on the possible roles of the *LFY* ortholog in leaf development in *M. truncatula*. At present, there are two hypotheses to interpret how the *LFY* orthologs replace *KNOXI* to promote indeterminacy in IRLC. One hypothesis is that *LFY* regulates the same target genes of *KNOXI*, and the other hypothesis is that *LFY* and *KNOXI* regulate parallel pathways (Champagne et al., 2007). Our data show that *OX-KNOXI* can increase leaf complexity probably through the conserved pathway. Should *SGL1* have the same regulatory mechanism as *KNOXI*, overexpression of *SGL1* would be able to promote indeterminacy in developing leaves. However, we were surprised to find that leaf complexity was not changed in *OX-SGL1* plants. These observations support the hypothesis that *KNOXI* and *LFY* regulate parallel pathways instead of regulating the same targets in IRLC.

The unexpected phenotypic output in response to the ectopic expression of *SGL1* raises a new question: Why does *OX-SGL1* fail to induce an increase in the degree of leaflet reiteration in *M. truncatula*? In tomato, overexpression of *KNOXI* in specific domains of developing leaves resulted in different leaf complexity, suggesting that *KNOXI* functions in a spatial- and temporal-dependent manner (Shani et al., 2009). It is possible that distinct leaf developmental windows exist in IRLC species, thus allowing *SGL1* to function in a specific stage or domain. On the other hand, *LFY* may function with its coregulator *UNUSUAL FLORAL ORGANS* (*UFO*) in leaf development of IRLC species. It has been shown that ectopic expression of *UFO* led to dissected leaves, similar to ectopic expression of *KNOXI* in *Arabidopsis* (Ingram et al., 1995; Lee et al., 1997). Moreover, the lobed leaf form requires *LFY* activity (Lee et al., 1997), indicating that *UFO* promotes indeterminacy in leaf development in a *LFY*-dependent manner. In addition, loss of function of *STAMINA PISTILLOIDA*, the ortholog of *UFO* in pea, led to a reduction of leaflet number (Taylor et al., 2001). Therefore, *UFO* orthologs may play an important role in recruiting *LFY* orthologs into compound leaf patterning in IRLC. Characterization of the loss-of-function *UFO* ortholog mutant in *M. truncatula* and a comparison of the phenotype and regulatory targets between *OX-SGL1* and *OX-UFO* may help to provide insight into the roles of the *UFO/LFY* cascade in compound leaf patterning.

METHODS

Plant Materials and Growth Conditions

Medicago truncatula (ecotype R108) plants were grown in the greenhouse at 22°C day/20°C night temperature, 16-h-day/8-h-night photoperiod, and 70 to 80% relative humidity. *Arabidopsis thaliana* (Landsberg *erecta*) plants were grown in a growth chamber at 20°C and a daylength of 18 h. The *Arabidopsis as1* allele (CS16272, ecotype Landsberg *erecta*) was obtained from TAIR.

Gene Constructs

To make the $PHAN_{RNAi}$ construct, a 390-bp fragment of *PHAN* was PCR amplified from wild-type *M. truncatula* and cloned into the pENTR/D-TOPO cloning vector (Invitrogen), then transferred into the pANDA35K vector by attL × attR recombination reactions (Invitrogen). To make the complementation construct, a 2611-bp *PHAN* promoter sequence plus 1080-bp *PHAN* coding sequence was PCR amplified and cloned into the pHGWFS7 vector (Karimi et al., 2002). To generate the *PHANpro:GUS* construct, a 2611-bp promoter region of *PHAN* was amplified and transferred into the pHGWFS7 vector (Karimi et al., 2002) for gene expression pattern analysis. For overexpression of *PHAN*, *KNOX1*, *KNOX2*, *KNOX4*, *KNOX6*, and *SGL1*, the CDS of these genes were amplified and cloned to the pEarleyGate 100 vector (Earley et al., 2006), respectively. Primer sequences are listed in Supplemental Table 3.

Stable Plant Transformation

Gene constructs were introduced into disarmed *Agrobacterium tumefaciens* using the freezing/heat shock method. *Agrobacterium* strain EHA105, harboring various vectors, was used for *M. truncatula* transformation as described (Cosson et al., 2006). The numbers of transgenic lines are listed in Supplemental Table 2.

GUS Staining and Scanning Electron Microscopy Analysis

GUS activities were histochemically detected as described previously (Zhou et al., 2011). For scanning electron microscopy, leaf tissue samples were first fixed in fixative solution (3% glutaraldehyde in 25 mM phosphate buffer, pH 7.0) overnight, dehydrated in graded ethanol series, and then critical point dried. The Hitachi TM-3000 scanning electron microscope was used for observation of samples at an accelerating voltage of 15 kV.

RNA Extraction, RT-PCR, Real-Time PCR Analysis, and Statistical Analysis

Total RNA from different organs, such as leaf, petiole, and shoot apices, was extracted from 4-week-old plants. RT-PCR and real-time PCR analysis were performed as described previously (Zhou et al., 2012). The single-factor ANOVA method was used to estimate if the difference is significant in analysis of gene expression level and plant phenotype.

RNA in Situ Hybridization

The 752-, 587-, 632-, 681-, and 777-bp fragments were isolated from the CDS of *PHAN*, *KNOX1*, *KNOX2*, *KNOX6*, and *KNOX7*, respectively. The PCR products were labeled with digoxigenin. RNA in situ hybridization was performed on shoot apices of 6-week-old plants as previously described (Zhou et al., 2011).

Phylogenetic Analysis

Alignment of multiple sequences was performed using ClustalW2 with default parameters (alignment type, slow; protein weight matrix, gonnet; Gap open, 10; Gap extension, 0.1). The neighbor-joining phylogenetic tree was constructed using the MEGA 6 software suite (http://www.megasoftware.net/). The most parsimonious trees with bootstrap values from 1000 trials were shown.

Accession Numbers

Sequence data from this article can be found in the National Center for Biotechnology Information GenBank under the following accession numbers: KNOX1, Medtr2g024390; KNOX2, Medtr1g017080; KNOX3, Medtr1g012960; KNOX4, Medtr5g011070; KNOX5, Medtr3g106400; KNOX6, Medtr5g085860; KNOX7, Medtr5g033720; KNOX8, Medtr1g084060; KNOX9, Medtr4g116545; KNOX10, Medtr2g461240; Mt-PHAN, Medtr7g061550; PHAN, CAA06612; CRI, AAG10600.1; Gm-PHANa, NP_001236839.1; Gm-PHANb, NP_001235251.1; Lj-PHANa, AAX21343.1; Lj-PHANb, AAX21344.1; AS1, NP_181299.1; and Ch-AS1, ABF59515.1.

Supplemental Data

The following materials are available in the online version of this article.

Supplemental Figure 1. Developmental Defects in Leaves of the *phan* Mutant.

Supplemental Figure 2. Transcript Levels of *YABBY* and *HD-ZIP III* Gene Families in *M. truncatula*.

Supplemental Figure 3. Developmental Defects in Flower Organs of the *phan* Mutant.

Supplemental Figure 4. Transcript Levels of *PHAN* in Wild Type and the *phan* Mutant.

Supplemental Figure 5. Alignment of ARP Proteins in Different Species.

Supplemental Figure 6. Expression Patterns of *PHAN* and Overexpression of *PHAN*.

Supplemental Figure 7. Phylogenetic Analysis of Members of *KNOX* Gene Family in *M. truncatula* and *Arabidopsis*.

Supplemental Figure 8. Expression Patterns of *KNOXI* Genes.

Supplemental Figure 9. Transcript Levels of *KNOX1*, *2*, and *6* in the Wild Type and *knox1*, *2*, and *6* Mutants.

Supplemental Figure 10. Genetic Interactions among *phan* and *knoxi* Mutants.

Supplemental Figure 11. Transcript Levels of *PHAN* in the Wild Type and *knox1*, *2*, and *6* Mutants.

Supplemental Figure 12. Flower Phenotype of the Wild Type, *phan*, *sgl1*, and *phan sgl1*.

Supplemental Figure 13. Summary of the Expression Patterns of *ARP* Genes among Species.

Supplemental Table 1. List of Mutant Alleles.

Supplemental Table 2. List of the Number of Transgenic Lines.

Supplemental Table 3. Primers Used in This Study.

Supplemental Data Set 1. Alignments Used to Generate the Phylogeny Presented in Supplemental Figure 2A.

Supplemental Data Set 2. Alignments Used to Generate the Phylogeny Presented in Supplemental Figure 2C.

Supplemental Data Set 3. Sequence Alignment Used to Generate the Phylogeny Presented in Figure 2D.

Supplemental Data Set 4. Sequence Alignment Used to Generate the Phylogeny Presented in Supplemental Figure 7.

ACKNOWLEDGMENTS

We thank Jackie Kelley and Amy Mason for critical reading of the article. We thank Kirankumar Mysore and Million Tadege for providing the *Tnt1* mutants; Eun Suk Jo for assistance with DNA extraction, tissue culture, and plant care; Jin Nakashima for anatomical analysis; and Tui Ray and Stacy Allen for real-time PCR analysis. We are grateful to the greenhouse staff for assistance with plant growth. This work was supported by The Samuel Roberts Noble Foundation, the BioEnergy Science Center, and the Natural Science Foundation of China (31371235). The BioEnergy Science Center is a U.S. Department of Energy Bioenergy Research Center supported by the Office of Biological and Environmental Research in the DOE Office of Science.

AUTHOR CONTRIBUTIONS

C.Z. and Z.-Y.W. designed the research. C.Z., L.H., G.L., M.C., C.F., and X.C. performed the experiments. C.Z., L.H., G.L., M.C., C.F., and X.C. analyzed the data. J.W. and Y.T. contributed analytical tools. C.Z. and Z.-Y.W. wrote the article.

Received February 2, 2014; revised March 31, 2014; accepted April 10, 2014; published April 29, 2014.

REFERENCES

Barkoulas, M., Hay, A., Kougioumoutzi, E., and Tsiantis, M. (2008). A developmental framework for dissected leaf formation in the Arabidopsis relative *Cardamine hirsuta*. Nat. Genet. **40:** 1136–1141.

Belles-Boix, E., Hamant, O., Witiak, S.M., Morin, H., Traas, J., and Pautot, V. (2006). KNAT6: an Arabidopsis homeobox gene involved in meristem activity and organ separation. Plant Cell **18:** 1900–1907.

Bharathan, G., Goliber, T.E., Moore, C., Kessler, S., Pham, T., and Sinha, N.R. (2002). Homologies in leaf form inferred from KNOXI gene expression during development. Science **296:** 1858–1860.

Bolduc, N., and Hake, S. (2009). The maize transcription factor KNOTTED1 directly regulates the gibberellin catabolism gene ga2ox1. Plant Cell **21:** 1647–1658.

Bolduc, N., Tyers, R., Freeling, M., and Hake, S. (2014). Unequal redundancy in maize knotted1 homeobox genes. Plant Physiol. **164:** 229–238.

Byrne, M.E., Barley, R., Curtis, M., Arroyo, J.M., Dunham, M., Hudson, A., and Martienssen, R.A. (2000). Asymmetric leaves1 mediates leaf patterning and stem cell function in Arabidopsis. Nature **408:** 967–971.

Byrne, M.E., Simorowski, J., and Martienssen, R.A. (2002). ASYMMETRIC LEAVES1 reveals knox gene redundancy in Arabidopsis. Development **129:** 1957–1965.

Champagne, C.E., Goliber, T.E., Wojciechowski, M.F., Mei, R.W., Townsley, B.T., Wang, K., Paz, M.M., Geeta, R., and Sinha, N.R. (2007). Compound leaf development and evolution in the legumes. Plant Cell **19:** 3369–3378.

Cosson, V., Durand, P., d'Erfurth, I., Kondorosi, A., and Ratet, P. (2006). *Medicago truncatula* transformation using leaf explants. Methods Mol. Biol. **343:** 115–127.

Di Giacomo, E., Sestili, F., Iannelli, M.A., Testone, G., Mariotti, D., and Frugis, G. (2008). Characterization of KNOX genes in *Medicago truncatula*. Plant Mol. Biol. **67:** 135–150.

Earley, K.W., Haag, J.R., Pontes, O., Opper, K., Juehne, T., Song, K., and Pikaard, C.S. (2006). Gateway-compatible vectors for plant functional genomics and proteomics. Plant J. **45:** 616–629.

Ge, L., Peng, J., Berbel, A., Madueño, F., and Chen, R. (2014). Regulation of compound leaf development by *PHANTASTICA* in *Medicago truncatula.* Plant Physiol. **164:** 216–228.

Guo, M., Thomas, J., Collins, G., and Timmermans, M.C. (2008). Direct repression of KNOX loci by the ASYMMETRIC LEAVES1 complex of Arabidopsis. Plant Cell **20:** 48–58.

Hake, S., Smith, H.M., Holtan, H., Magnani, E., Mele, G., and Ramirez, J. (2004). The role of knox genes in plant development. Annu. Rev. Cell Dev. Biol. **20:** 125–151.

Hareven, D., Gutfinger, T., Parnis, A., Eshed, Y., and Lifschitz, E. (1996). The making of a compound leaf: genetic manipulation of leaf architecture in tomato. Cell **84:** 735–744.

Hay, A., and Tsiantis, M. (2006). The genetic basis for differences in leaf form between *Arabidopsis thaliana* and its wild relative *Cardamine hirsuta*. Nat. Genet. **38:** 942–947.

Hay, A., and Tsiantis, M. (2010). KNOX genes: versatile regulators of plant development and diversity. Development **137:** 3153–3165.

Hay, A., Barkoulas, M., and Tsiantis, M. (2006). ASYMMETRIC LEAVES1 and auxin activities converge to repress BREVIPEDICELLUS expression and promote leaf development in Arabidopsis. Development **133:** 3955–3961.

Hofer, J., Gourlay, C., Michael, A., and Ellis, T.H. (2001). Expression of a class 1 knotted1-like homeobox gene is down-regulated in pea compound leaf primordia. Plant Mol. Biol. **45:** 387–398.

Hofer, J., Turner, L., Hellens, R., Ambrose, M., Matthews, P., Michael, A., and Ellis, N. (1997). UNIFOLIATA regulates leaf and flower morphogenesis in pea. Curr. Biol. **7:** 581–587.

Ingram, G.C., Goodrich, J., Wilkinson, M.D., Simon, R., Haughn, G.W., and Coen, E.S. (1995). Parallels between UNUSUAL FLORAL ORGANS and FIMBRIATA, genes controlling flower development in Arabidopsis and Antirrhinum. Plant Cell **7:** 1501–1510.

Jasinski, S., Piazza, P., Craft, J., Hay, A., Woolley, L., Rieu, I., Phillips, A., Hedden, P., and Tsiantis, M. (2005). KNOX action in Arabidopsis is mediated by coordinate regulation of cytokinin and gibberellin activities. Curr. Biol. **15:** 1560–1565.

Karimi, M., Inzé, D., and Depicker, A. (2002). GATEWAY vectors for Agrobacterium-mediated plant transformation. Trends Plant Sci. **7:** 193–195.

Kim, M., McCormick, S., Timmermans, M., and Sinha, N. (2003a). The expression domain of *PHANTASTICA* determines leaflet placement in compound leaves. Nature **424:** 438–443.

Kim, M., Pham, T., Hamidi, A., McCormick, S., Kuzoff, R.K., and Sinha, N. (2003b). Reduced leaf complexity in tomato wiry mutants suggests a role for PHAN and KNOX genes in generating compound leaves. Development **130:** 4405–4415.

Lee, I., Wolfe, D.S., Nilsson, O., and Weigel, D. (1997). A LEAFY co-regulator encoded by UNUSUAL FLORAL ORGANS. Curr. Biol. **7:** 95–104.

Lincoln, C., Long, J., Yamaguchi, J., Serikawa, K., and Hake, S. (1994). A knotted1-like homeobox gene in Arabidopsis is expressed in the vegetative meristem and dramatically alters leaf morphology when overexpressed in transgenic plants. Plant Cell **6:** 1859–1876.

Lodha, M., Marco, C.F., and Timmermans, M.C. (2013). The ASYMMETRIC LEAVES complex maintains repression of KNOX homeobox genes via direct recruitment of Polycomb-repressive complex2. Genes Dev. **27:** 596–601.

Long, J.A., Moan, E.I., Medford, J.I., and Barton, M.K. (1996). A member of the KNOTTED class of homeodomain proteins encoded by the STM gene of Arabidopsis. Nature **379:** 66–69.

Luo, J.H., Yan, J., Weng, L., Yang, J., Zhao, Z., Chen, J.H., Hu, X.H., and Luo, D. (2005). Different expression patterns of duplicated PHANTASTICA-like genes in *Lotus japonicus* suggest their divergent functions during compound leaf development. Cell Res. **15:** 665–677.

Mishra, R.K., Chaudhary, S., Kumar, A., and Kumar, S. (2009). Effects of MULTIFOLIATE-PINNA, AFILA, TENDRIL-LESS and UNIFOLIATA genes on leafblade architecture in *Pisum sativum*. Planta **230:** 177–190.

Moon, J., and Hake, S. (2011). How a leaf gets its shape. Curr. Opin. Plant Biol. **14:** 24–30.

Ori, N., Eshed, Y., Chuck, G., Bowman, J.L., and Hake, S. (2000). Mechanisms that control knox gene expression in the Arabidopsis shoot. Development **127:** 5523–5532.

Ragni, L., Belles-Boix, E., Günl, M., and Pautot, V. (2008). Interaction of KNAT6 and KNAT2 with BREVIPEDICELLUS and PENNYWISE in Arabidopsis inflorescences. Plant Cell **20:** 888–900.

Sakamoto, T., Kamiya, N., Ueguchi-Tanaka, M., Iwahori, S., and Matsuoka, M. (2001). KNOX homeodomain protein directly suppresses the expression of a gibberellin biosynthetic gene in the tobacco shoot apical meristem. Genes Dev. **15:** 581–590.

Schneeberger, R., Tsiantis, M., Freeling, M., and Langdale, J.A. (1998). The rough sheath2 gene negatively regulates homeobox gene expression during maize leaf development. Development **125:** 2857–2865.

Semiarti, E., Ueno, Y., Tsukaya, H., Iwakawa, H., Machida, C., and Machida, Y. (2001). The ASYMMETRIC LEAVES2 gene of *Arabidopsis thaliana* regulates formation of a symmetric lamina, establishment of venation and repression of meristem-related homeobox genes in leaves. Development **128:** 1771–1783.

Serikawa, K.A., Martinez-Laborda, A., Kim, H.S., and Zambryski, P.C. (1997). Localization of expression of KNAT3, a class 2 knotted1-like gene. Plant J. **11:** 853–861.

Serrano-Cartagena, J., Robles, P., Ponce, M.R., and Micol, J.L. (1999). Genetic analysis of leaf form mutants from the Arabidopsis Information Service collection. Mol. Gen. Genet. **261:** 725–739.

Shani, E., Burko, Y., Ben-Yaakov, L., Berger, Y., Amsellem, Z., Goldshmidt, A., Sharon, E., and Ori, N. (2009). Stage-specific regulation of *Solanum lycopersicum* leaf maturation by class 1 KNOTTED1-LIKE HOMEOBOX proteins. Plant Cell **21:** 3078–3092.

Tadege, M., Wen, J., He, J., Tu, H., Kwak, Y., Eschstruth, A., Cayrel, A., Endre, G., Zhao, P.X., Chabaud, M., Ratet, P., and Mysore, K.S. (2008). Large-scale insertional mutagenesis using the *Tnt1* retrotransposon in the model legume *Medicago truncatula.* Plant J. **54:** 335–347.

Tattersall, A.D., Turner, L., Knox, M.R., Ambrose, M.J., Ellis, T.H., and Hofer, J.M. (2005). The mutant crispa reveals multiple roles for PHANTASTICA in pea compound leaf development. Plant Cell **17:** 1046–1060.

Taylor, S., Hofer, J., and Murfet, I. (2001). Stamina pistilloida, the pea ortholog of Fim and UFO, is required for normal development of flowers, inflorescences, and leaves. Plant Cell **13:** 31–46.

Theodoris, G., Inada, N., and Freeling, M. (2003). Conservation and molecular dissection of ROUGH SHEATH2 and ASYMMETRIC LEAVES1 function in leaf development. Proc. Natl. Acad. Sci. USA **100:** 6837–6842.

Timmermans, M.C., Hudson, A., Becraft, P.W., and Nelson, T. (1999). ROUGH SHEATH2: a Myb protein that represses knox homeobox genes in maize lateral organ primordia. Science **284:** 151–153.

Townsley, B.T., and Sinha, N.R. (2012). A new development: evolving concepts in leaf ontogeny. Annu. Rev. Plant Biol. **63:** 535–562.

Tsiantis, M., Schneeberger, R., Golz, J.F., Freeling, M., and Langdale, J.A. (1999). The maize rough sheath2 gene and leaf development programs in monocot and dicot plants. Science **284:** 154–156.

Tsuda, K., Ito, Y., Sato, Y., and Kurata, N. (2011). Positive autoregulation of a KNOX gene is essential for shoot apical meristem maintenance in rice. Plant Cell **23:** 4368–4381.

Venglat, S.P., Dumonceaux, T., Rozwadowski, K., Parnell, L., Babic, V., Keller, W., Martienssen, R., Selvaraj, G., and Datla, R. (2002). The homeobox gene BREVIPEDICELLUS is a key regulator of inflorescence architecture in Arabidopsis. Proc. Natl. Acad. Sci. USA **99:** 4730–4735.

Vollbrecht, E., Veit, B., Sinha, N., and Hake, S. (1991). The developmental gene Knotted-1 is a member of a maize homeobox gene family. Nature **350:** 241–243.

Waites, R., Selvadurai, H.R., Oliver, I.R., and Hudson, A. (1998). The PHANTASTICA gene encodes a MYB transcription factor involved in growth and dorsoventrality of lateral organs in Antirrhinum. Cell **93:** 779–789.

Wang, H., Chen, J., Wen, J., Tadege, M., Li, G., Liu, Y., Mysore, K.S., Ratet, P., and Chen, R. (2008). Control of compound leaf development by *FLORICAULA/LEAFY* ortholog *SINGLE LEAFLET1* in *Medicago truncatula.* Plant Physiol. **146:** 1759–1772.

Wojciechowski, M.F., Lavin, M., and Sanderson, M.J. (2004). A phylogeny of legumes (Leguminosae) based on analysis of the plastid matK gene resolves many well-supported subclades within the family. Am. J. Bot. **91:** 1846–1862.

Yanai, O., Shani, E., Dolezal, K., Tarkowski, P., Sablowski, R., Sandberg, G., Samach, A., and Ori, N. (2005). Arabidopsis KNOXI proteins activate cytokinin biosynthesis. Curr. Biol. **15:** 1566–1571.

Zhou, C., Han, L., Fu, C., Chai, M., Zhang, W., Li, G., Tang, Y., and Wang, Z.Y. (2012). Identification and characterization of *petiolule-like pulvinus* mutants with abolished nyctinastic leaf movement in the model legume *Medicago truncatula.* New Phytol. **196:** 92–100.

Zhou, C., Han, L., Hou, C., Metelli, A., Qi, L., Tadege, M., Mysore, K.S., and Wang, Z.Y. (2011). Developmental analysis of a *Medicago truncatula smooth leaf margin1* mutant reveals context-dependent effects on compound leaf development. Plant Cell **23:** 2106–2124.

Zoulias, N., Koenig, D., Hamidi, A., McCormick, S., and Kim, M. (2012). A role for PHANTASTICA in medio-lateral regulation of adaxial domain development in tomato and tobacco leaves. Ann. Bot. (Lond.) **109:** 407–418.

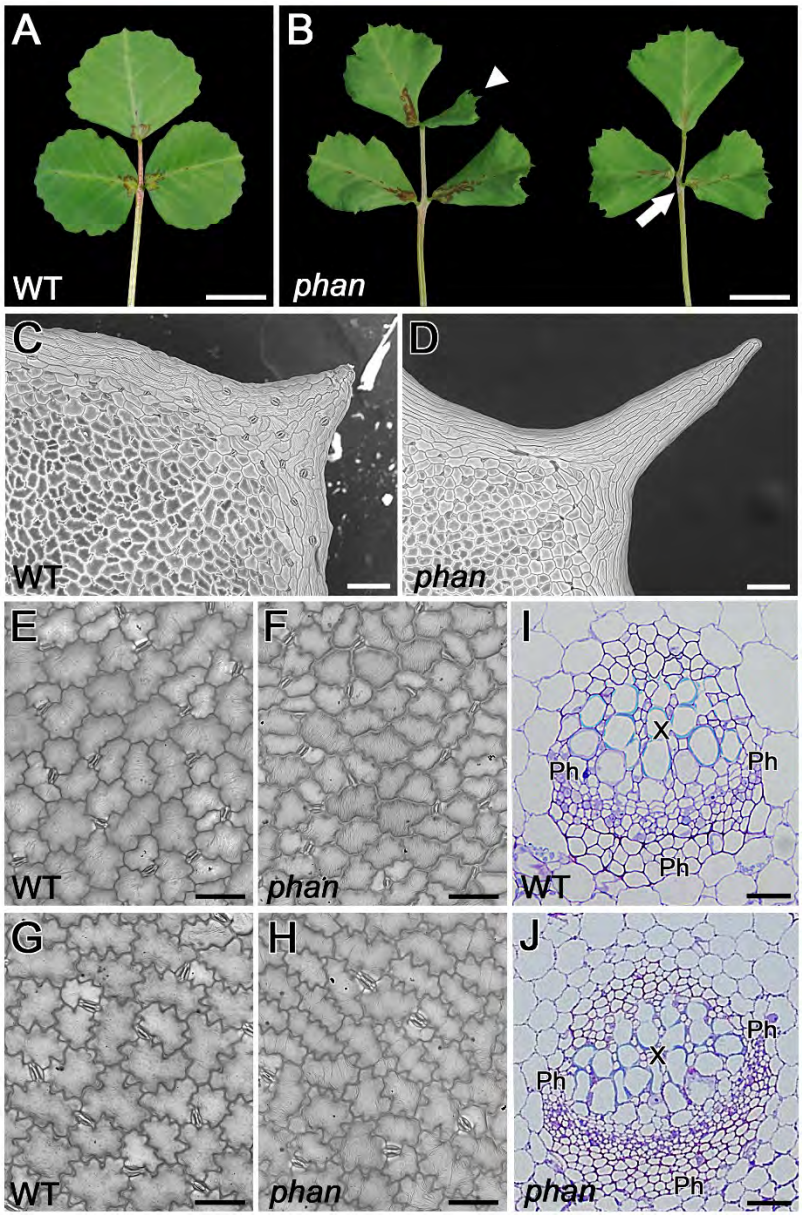

Supplemental Figure 1. Developmental Defects in Leaves of the *phan* Mutant.
(A) Wild type leaf.
(B) *phan* leaves. Arrowhead points to the ectopic terminal leaflet. Arrow indicates lateral leaflets developed on petiole in an asymmetric pattern.
(C) and (D) Scanning electron microscope images of leaf marginal tips of wild type (C) and *phan* (D).
(E) to (H) Scanning electron microscope images of epidermal cells of the adaxial side (E and F) and the abaxial side (G and H) of leaves in the wild type and *phan*.
(I) and (J) Transverse sections of vascular bundles in petioles of wild type and *phan*. Ph: phloem; X: xylem.
Bars = 1 cm in (A) and (B), 100 μm in (C) and (D), 50 μm in (E) to (H), and 20 μm in (I) and (J).

1

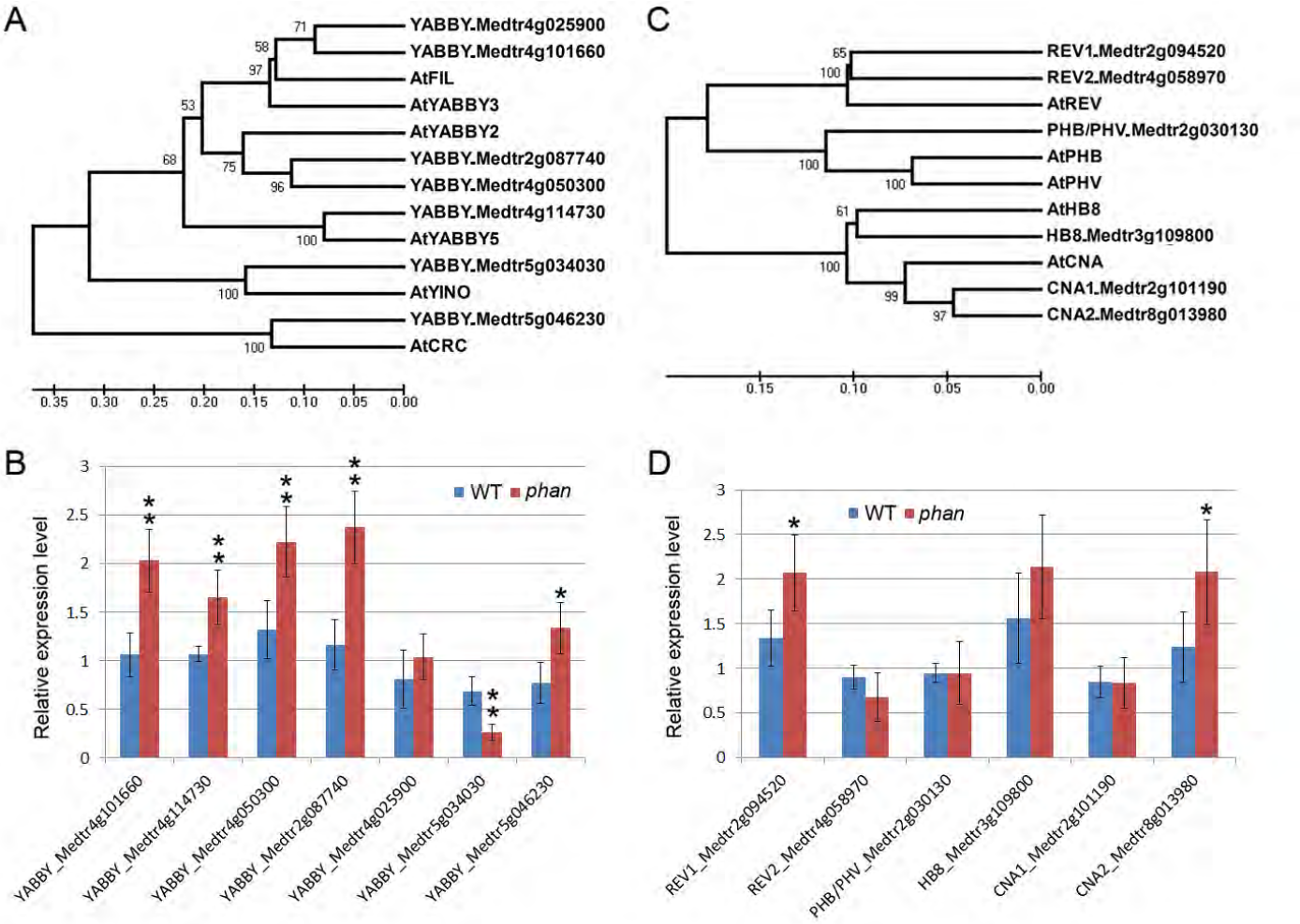

Supplemental Figure 2. Transcript Levels of *YABBY* and *HD-ZIP III* Gene Families in *M. truncatula*.

(A) Phylogenetic analysis of members of *YABBY* gene family in *M. truncatula* and *Arabidopsis.*

(B) Expression levels of *YABBY* genes in the vegetative buds of the wild type and *phan* mutant.

(C) Phylogenetic analysis of members of the *HD-ZIP III* gene family in *M. truncatula* and *Arabidopsis.*

(D) Expression levels of *HD-ZIP III* genes in the vegetative buds of the wild type and *phan* mutant.

Values are the means and SD of three biological replicates. *P < 0.05; **P < 0.01. The data were analyzed by single factor analysis of variance. The alignments used to generate the phylogenies in A and C are presented in Supplemental Datasets 1 and 2 online, respectively.

The scale bar in (A) and (C) indicates the sequence divergence is 0.05 per unit bar, which represent 5% substitutions per nucleotide position.

2

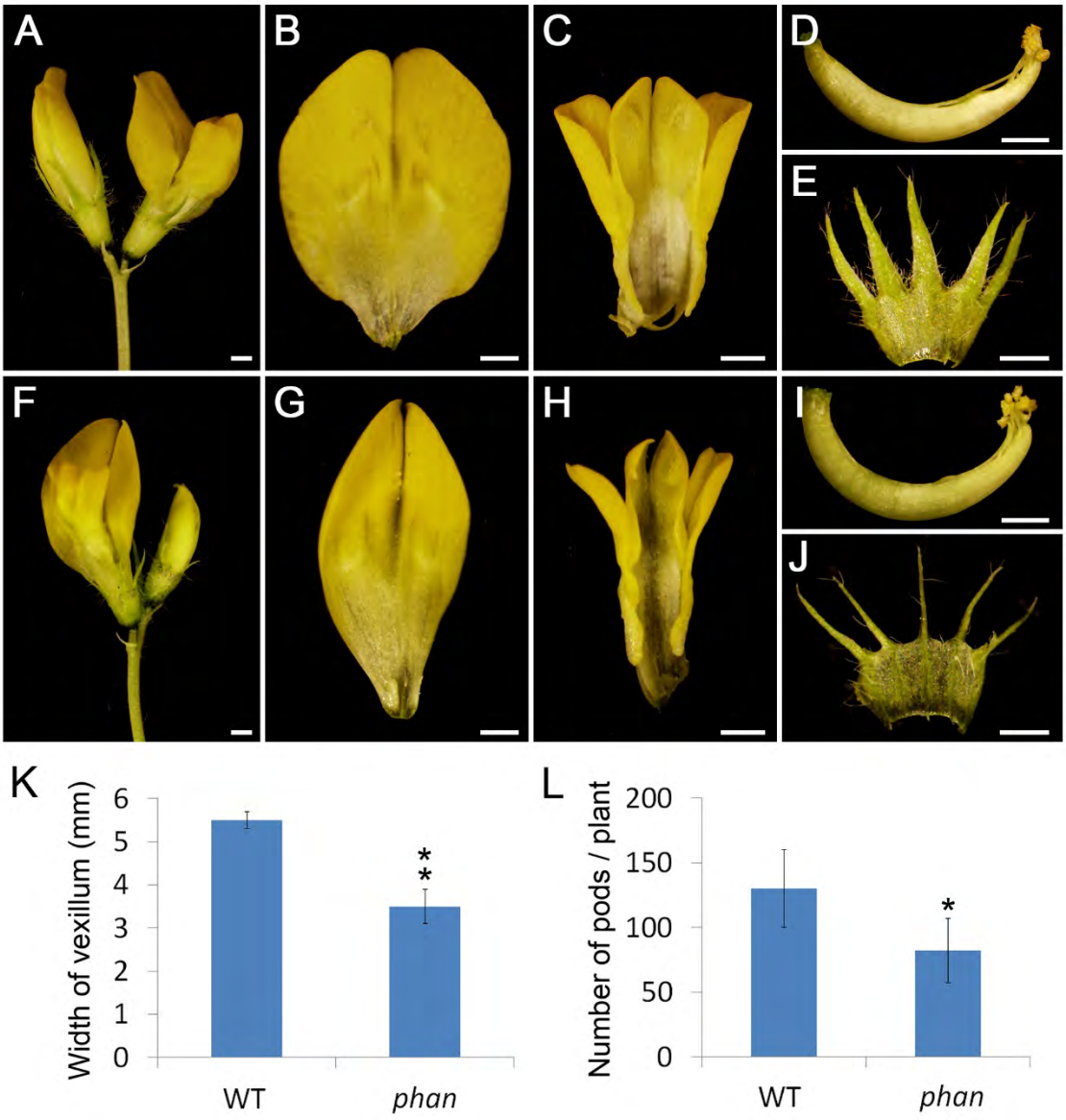

Supplemental Figure 3. Developmental Defects in Flower Organs of the *phan* Mutant.
(A) Flower phenotype in wild type.
(B) to (E) Dissected floral organs of the wild type, including vexillum (B), alae and keel (C), central carpel (D) and sepal (E).
(F) Flower phenotype in *phan*.
(G) to (J) Dissected floral organs of *phan*, including vexillum (G), alae and keel (H), central carpel (I) and sepal (J).
(K) Width of vexillum in the wild type and *phan*. Values shown are means ± SD; $n = 10$.
(L) Seed pod number in the wild type and *phan*. Values shown are means ± SD; $n = 5$.
*$P < 0.05$; **$P < 0.01$. The data were analyzed by single factor analysis of variance. Bars = 1 mm in (A) to (J).

3

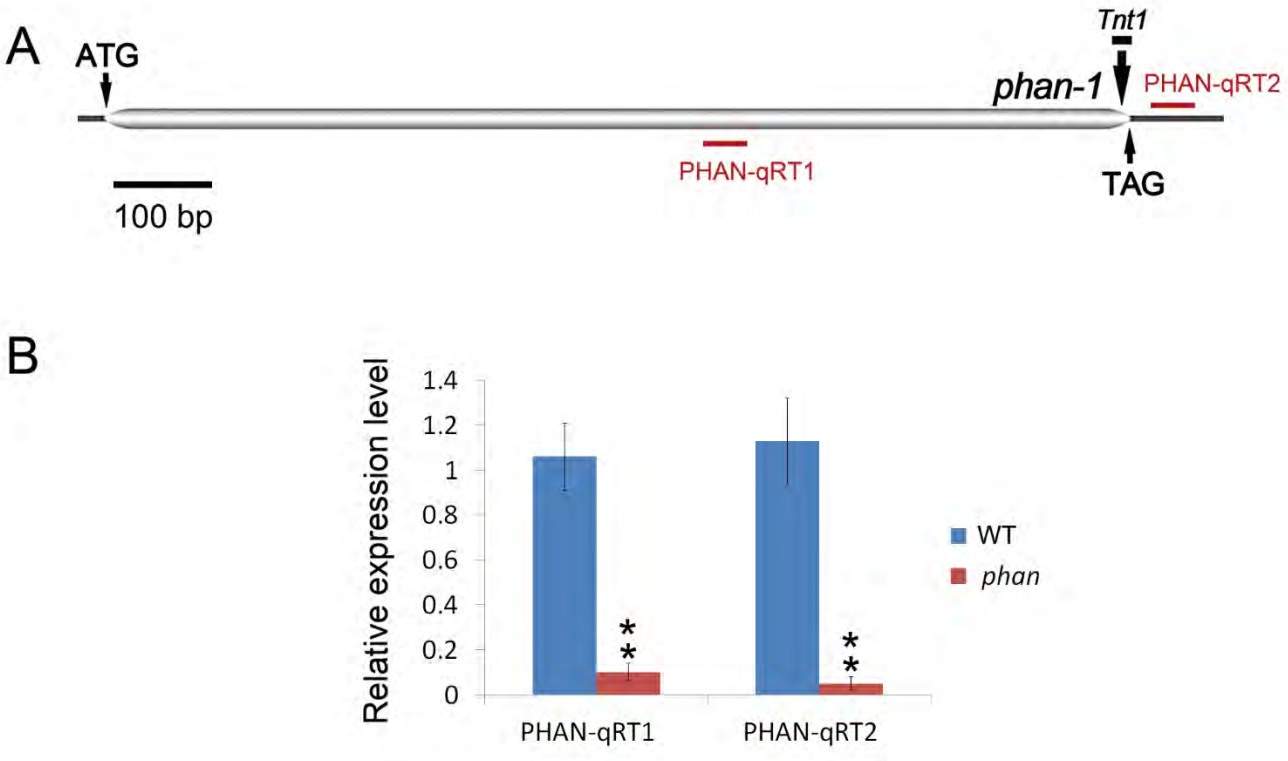

Supplemental Figure 4. Transcript Levels of *PHAN* in the Wild Type and the *phan* Mutant.
(A) Locations of amplification fragments by qRT-PCR. The PHAN-qRT1 fragment was amplified using primers upstream of the *Tnt1* insertion site. The PHAN-qRT2 fragment was amplified using primers downstream of the *Tnt1* insertion site.
(B) Transcript levels of *PHAN* in vegetative buds measured by qRT-PCR. Values are the means and SD of three biological replicates. **P < 0.01. The data were analyzed by single factor analysis of variance.

4

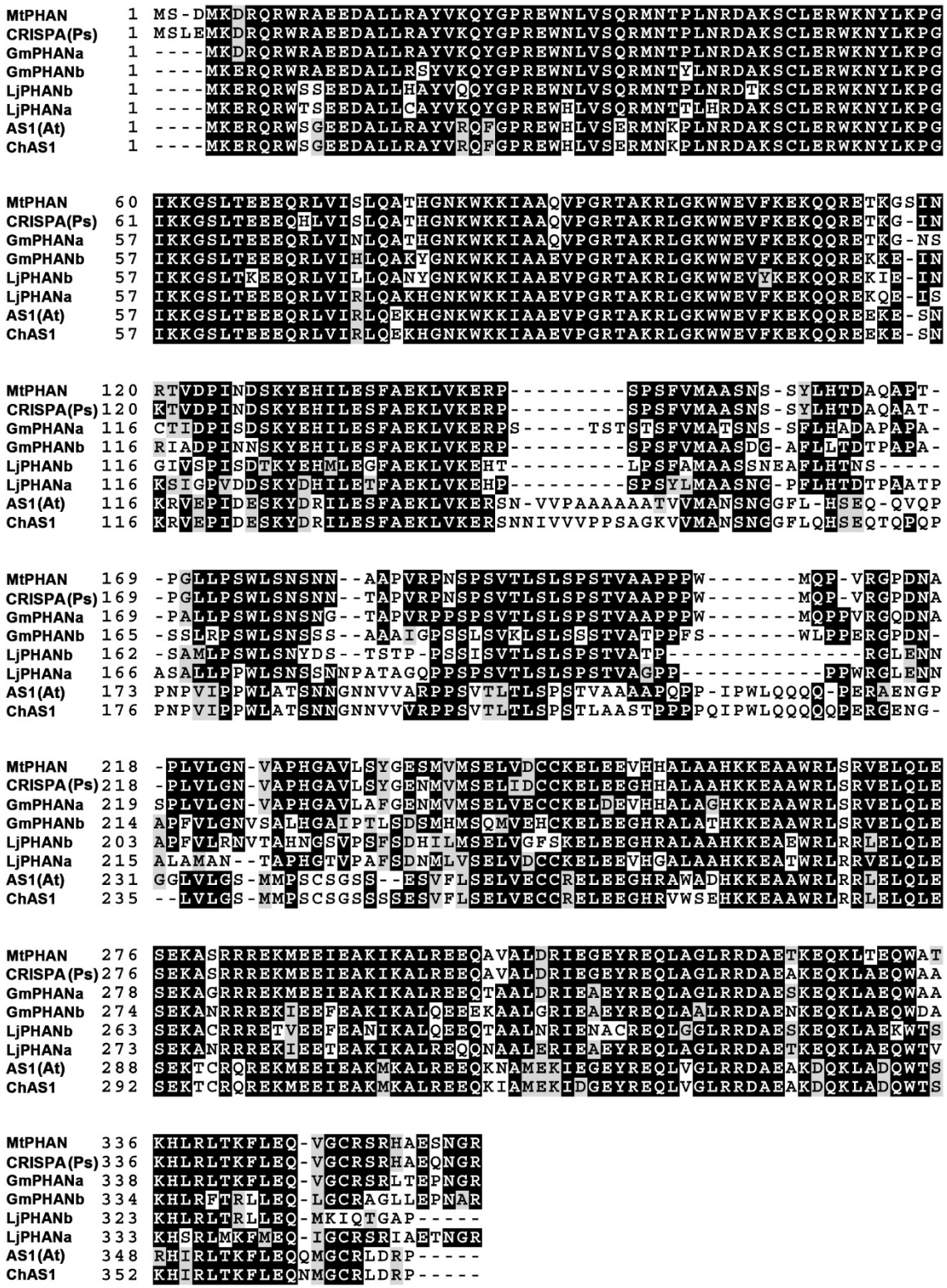

Supplemental Figure 5. Alignment of ARP Proteins in Different Species.
Alignment of ARP proteins in *Medicago truncatula* (Mt), *Pisum sativum* (Ps), *Glycine max* (Gm), *Lotus japonicas* (Lj), *Arabidopsis thaliana* (At) and *Cardamine hirsuta* (Ch).

5

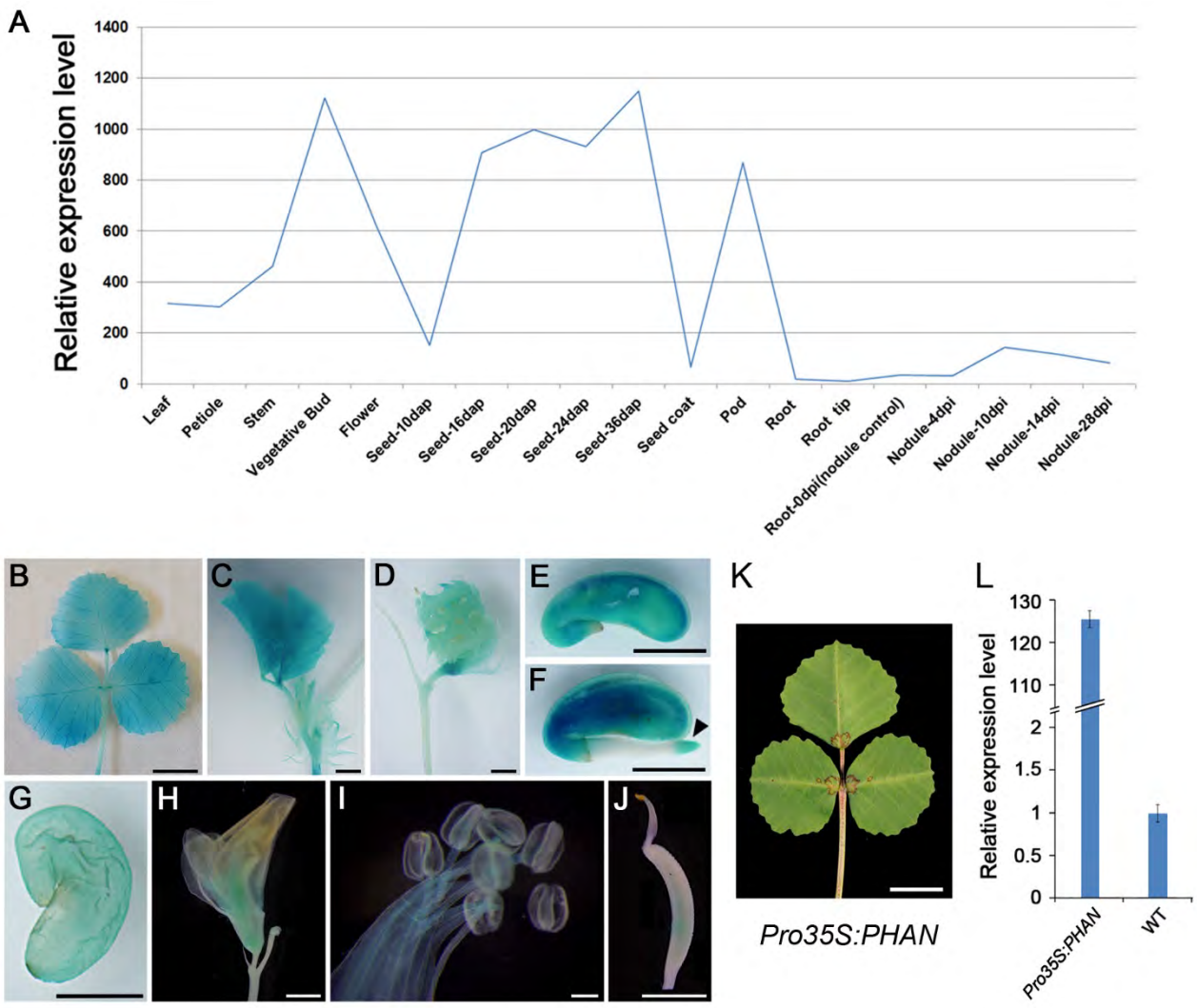

Supplemental Figure 6. Expression Patterns of *PHAN* and Overexpression of *PHAN*.

(A) The expression pattern of *PHAN* (probe set *Mtr.40836.1.S1_at*) in different organs.

(B) to (J) Promoter-GUS fusion studies of *PHAN* expression in transgenic plants. *PHAN* promoter driven GUS is expressed in the adult leaf (B), leaf buds (C), seed pod (D), seeds (E), root tip (F), seed coat (G) and different floral organs (H) to (J), such as filaments (I) and central carpel (J). Arrowhead points to the root tip of a germinating seed in (F).

(K) and (L) Overexpression of *PHAN* in *M. truncatula*. A representative leaf of *Pro35S:PHAN* transgenic plants is shown in (K). Transcript levels of *PHAN* in wild-type and *Pro35S:PHAN* transgenic plants are shown in (L).

Bars = 1 cm in (B) and (K), 2 mm in (C) to (H), and (J), and 200 μm in (I).

6

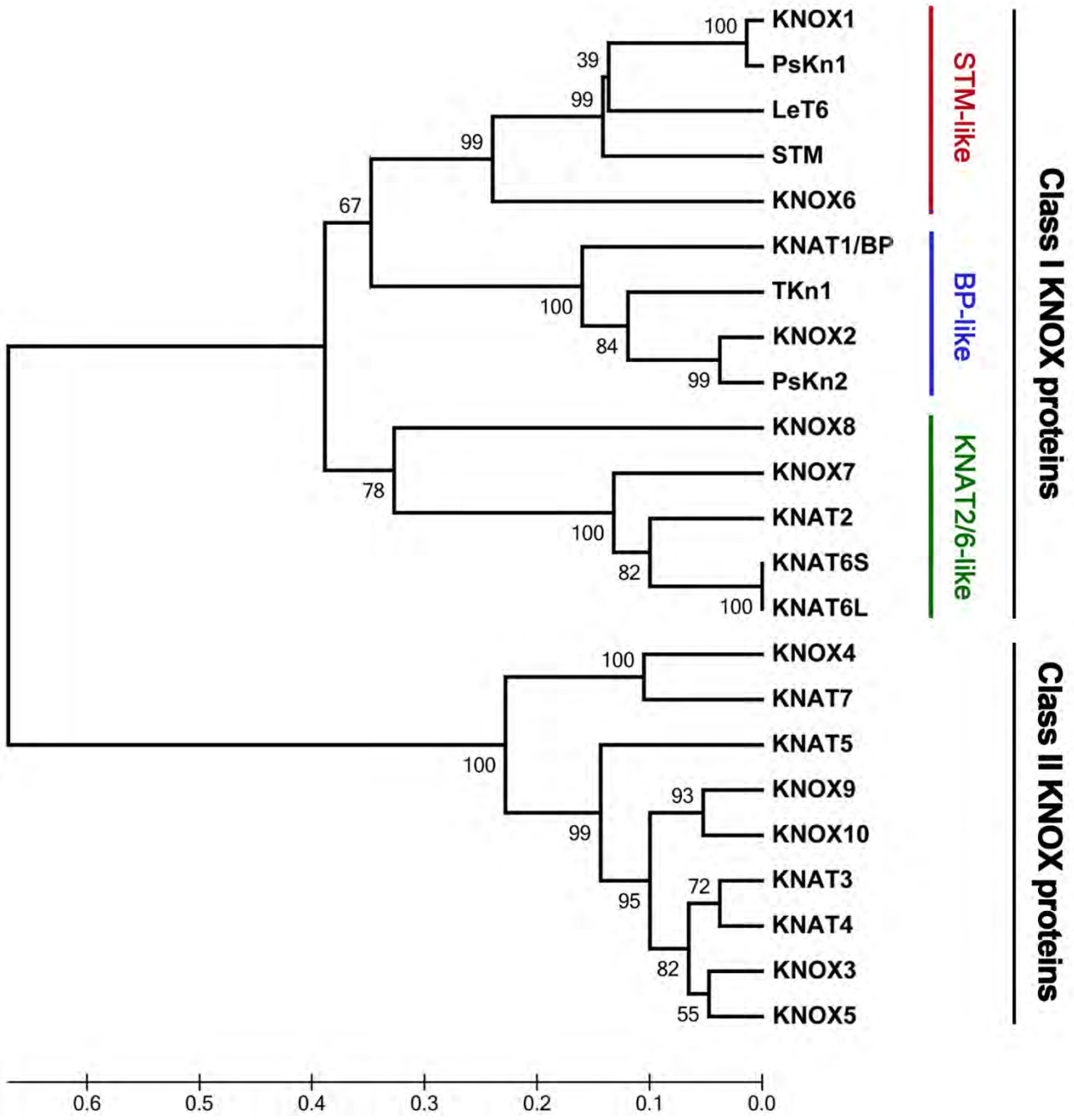

Supplemental Figure 7. Phylogenetic Analysis of Members of *KNOX* Gene Family in *M. truncatula* and *Arabidopsis*. *KNOX1*, *KNOX2*, *KNOX6*, *KNOX7* and *KNOX8* are class I *KNOX* genes. *KNOX3*, *KNOX4*, *KNOX5*, *KNOX9* and *KNOX10* are class II *KNOX* genes. Alignments used to generate the phylogeny are presented in Supplemental Dataset 4 online. The scale bar indicates the sequence divergence is 0.1 per unit bar, which represent 10% substitutions per nucleotide position.

7

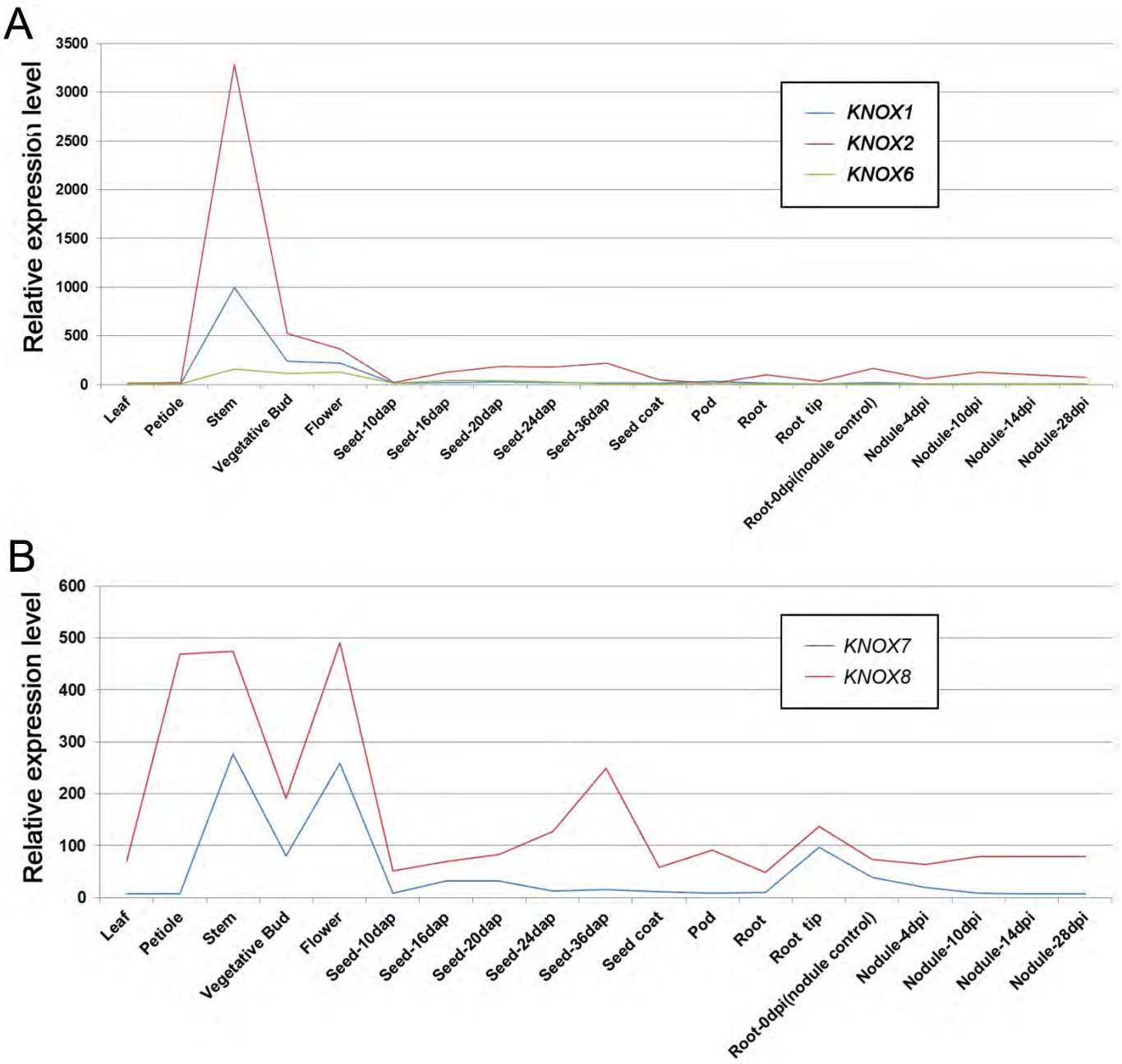

Supplemental Figure 8. Expression Patterns of *KNOXI* Genes.

(A) Expression profile of *KNOX1* (probe set *Mtr.13772.1.S1_at*), *KNOX2* (probe set *Mtr.9504.1.S1_at*) and *KNOX6* (probe set *Mtr.32410.1.S1_at*) transcripts.

(B) Expression profile of *KNOX7* (probe set *Mtr.36907.1.S1_at*) and *KNOX8* (probe set *Mtr.5446.1.S1_at*) transcripts.

8

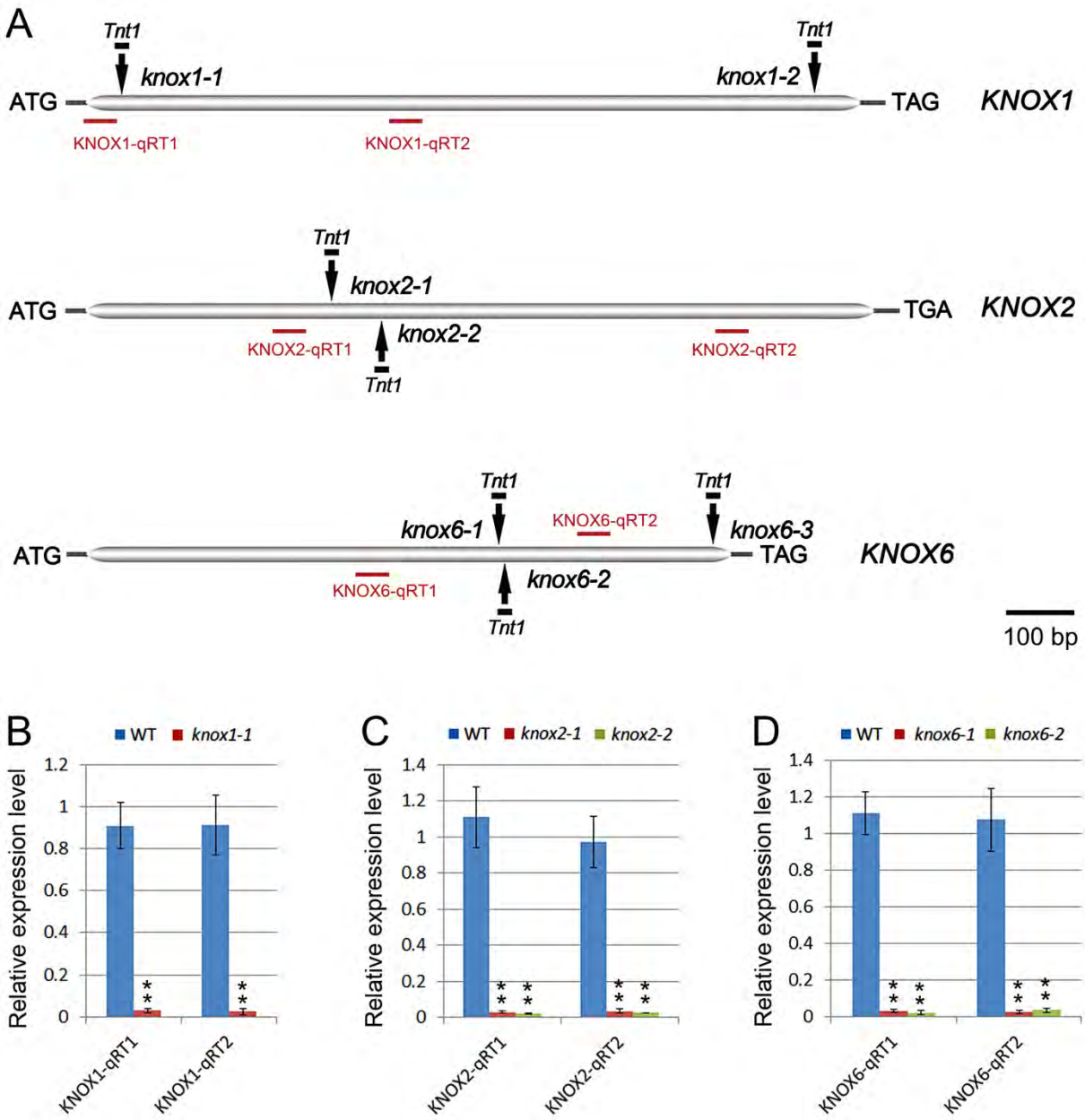

Supplemental Figure 9. Transcript Levels of *KNOX1*, *2* and *6* in the Wild Type and *knox1*, *2* and *6* Mutants.
(A) Locations of qRT-PCR amplification fragments upstream (-qRT1) and downstream (-qRT2) of the *Tnt1* insertion sites in the coding sequences of *KNOX1, 2* and *6*.
(B) to (D) Transcript levels of *KNOX1* (B), *KNOX2* (C) and *KNOX6* (D) in the vegetative buds of the wild type and mutants. Values are the means and SD of three biological replicates. **P < 0.01. The data were analyzed by single factor analysis of variance.

9

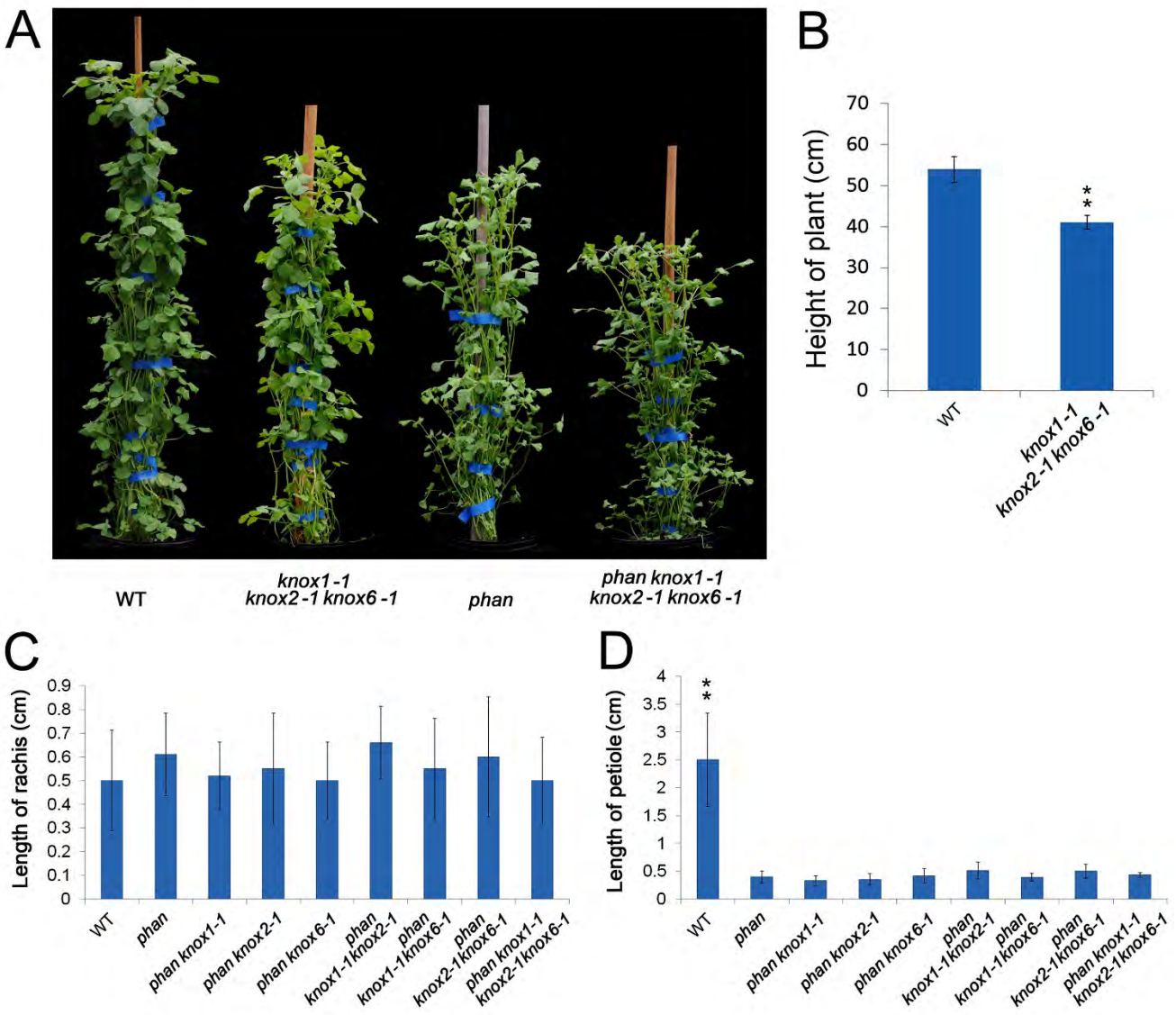

Supplemental Figure 10. Genetic Interactions among *phan* and *knoxi* Mutants.

(A) Sixty-day-old plants of the wild type, *knox1-1 knox2-1 knox6-1* triple mutant, *phan* single mutant and *phan knox1-1 knox2-1 knox6-1* quadruple mutant.

(B) Height of 60-day-old plants of the wild type and *knox1-1 knox2-1 knox6-1* triple mutant. Numbers are presented as means ± SD (*n* = 10). **P < 0.01.

(C) and (D) Lengths of the rachis (C) and petiole (D) in the wild type and mutants from different cross combinations. Numbers are presented as means ± SD (*n* = 10). **P < 0.01. The data were analyzed by single factor analysis of variance.

10

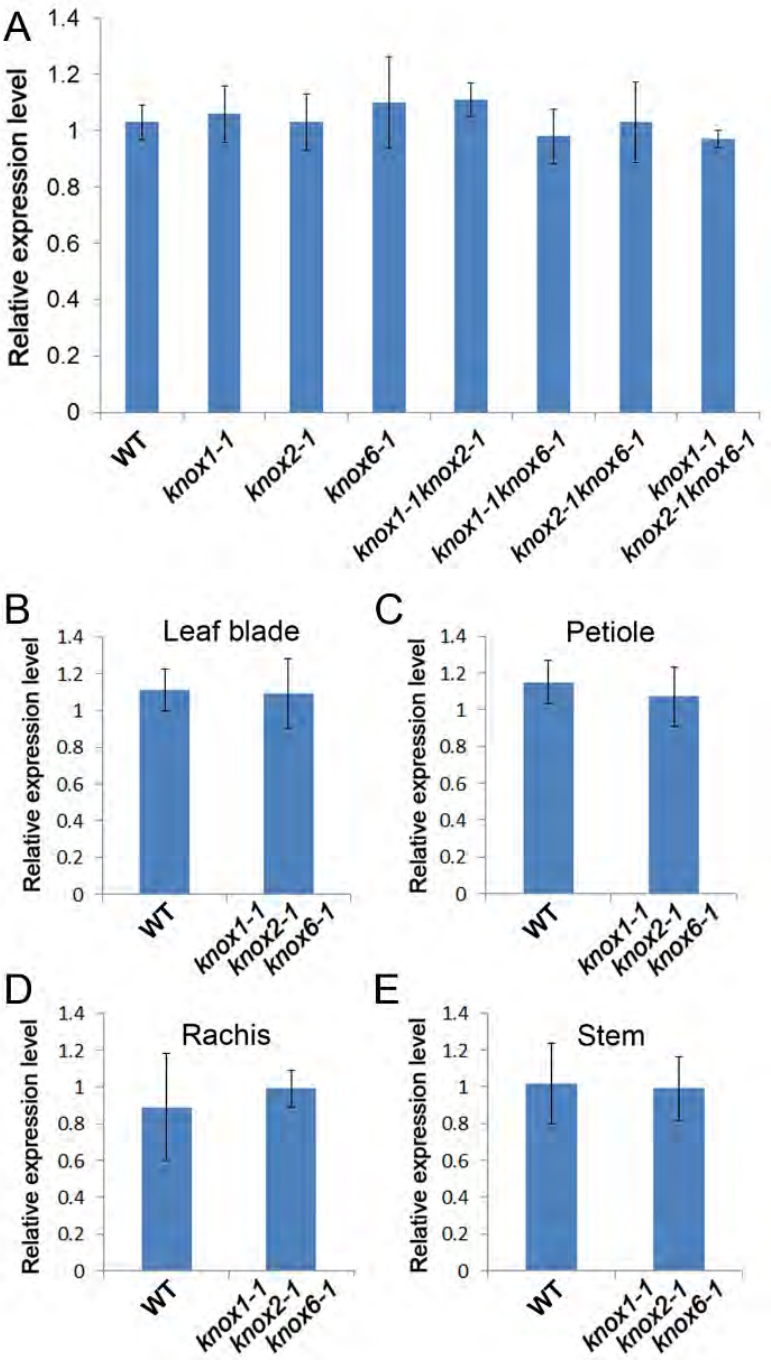

Supplemental Figure 11. Transcript Levels of *PHAN* in the Wild Type and *knox1*, *2* and *6* Mutants.
(A) Transcript level of *PHAN* in vegetative buds of the wild type and *knox1*, *2*, *6* single, double, and triple mutants.
(B) to (E) Transcript level of *PHAN* in the leaf blade (B), petiole (C), rachis (D), and stem (E) in the wild type and *knox1*, *2*, *6* triple mutant.
Values are the means and SD of three biological replicates.

11

Supplemental Figure 12. Flower Phenotype of the Wild Type, *phan*, *sgl1* and *phan sgl1*.
Bars = 3 mm.

12

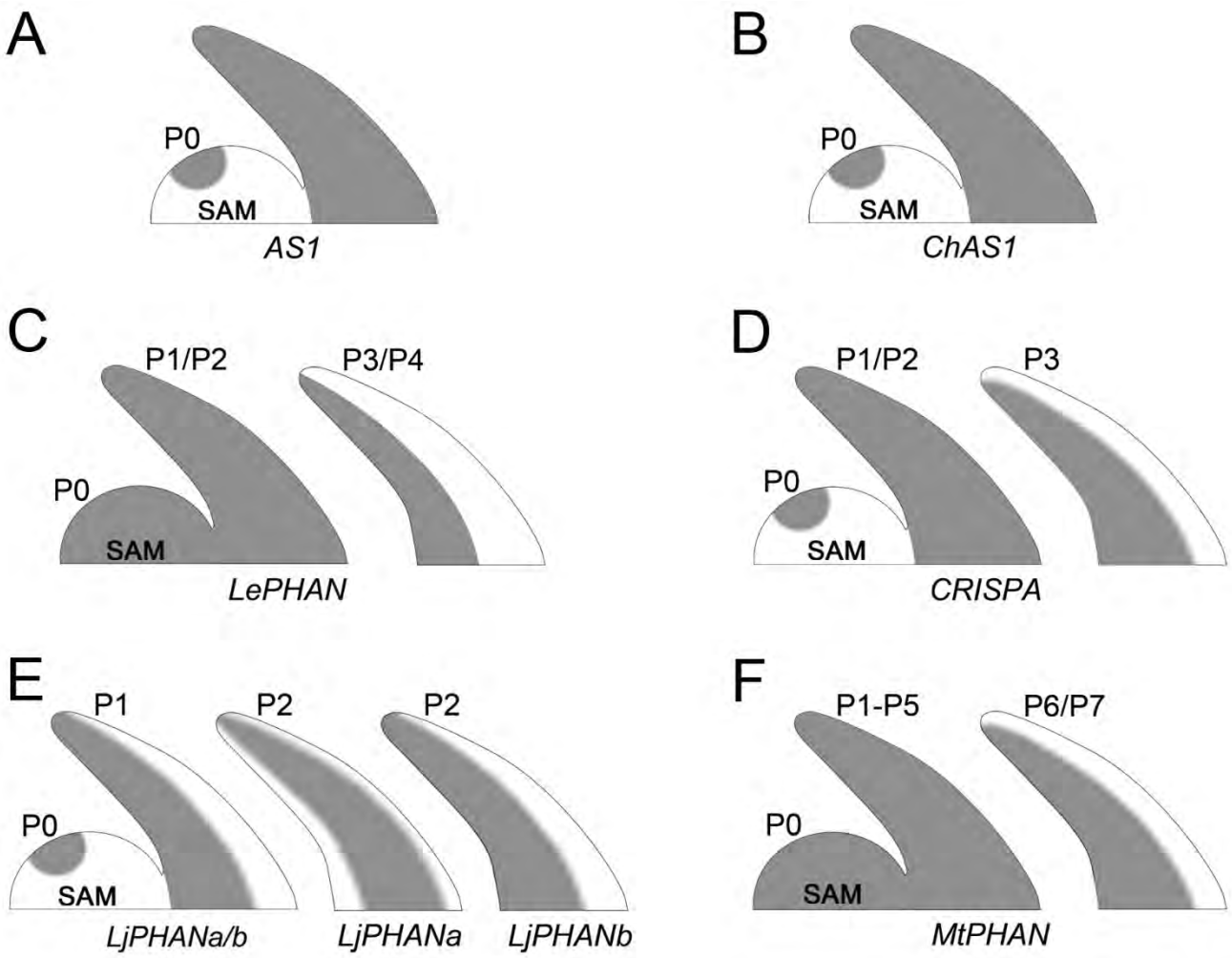

Supplemental Figure 13. Summary of the Expression Patterns of *ARP* Genes Among Species.
The expression domain (grey) of *ARP* genes is shown in *Arabidopsis* (A) (Byrne et al. 2000) , *Cardamine hirsuta* (B) (Hay and Tsiantis 2006), *Lycopersicon esculentum* (C) (Kim et al. 2003a; Kim et al. 2003b), *Pisum sativumv* (D) (Tattersall et al. 2005), *Lotus japonicas* (E) (Luo et al. 2005) and *Medicago truncatula* (F).

13

Supplemental References

Byrne ME, Barley R, Curtis M, Arroyo JM, Dunham M, Hudson A, Martienssen RA. 2000. Asymmetric leaves1 mediates leaf patterning and stem cell function in Arabidopsis. *Nature* **408**: 967-971.

Hay A, Tsiantis M. 2006. The genetic basis for differences in leaf form between Arabidopsis thaliana and its wild relative Cardamine hirsuta. *Nat Genet* **38**: 942-947.

Kim M, McCormick S, Timmermans M, Sinha N. 2003a. The expression domain of *PHANTASTICA* determines leaflet placement in compound leaves. *Nature* **424**: 438-443.

Kim M, Pham T, Hamidi A, McCormick S, Kuzoff RK, Sinha N. 2003b. Reduced leaf complexity in tomato wiry mutants suggests a role for PHAN and KNOX genes in generating compound leaves. *Development* **130**: 4405-4415.

Luo JH, Yan J, Weng L, Yang J, Zhao Z, Chen JH, Hu XH, Luo D. 2005. Different expression patterns of duplicated PHANTASTICA-like genes in Lotus japonicus suggest their divergent functions during compound leaf development. *Cell Res* **15**: 665-677.

Tattersall AD, Turner L, Knox MR, Ambrose MJ, Ellis TH, Hofer JM. 2005. The mutant crispa reveals multiple roles for PHANTASTICA in pea compound leaf development. *Plant Cell* **17**: 1046-1060.

14

Supplemental Table 1. List of Mutant Alleles

Gene	Mutant allele	Location of *Tnt1*	Flanking sequence of *Tnt1*
PHAN	*phan-1*	2nd exon	CATGCTGA (***Tnt1***) ATCAAATG
KNOX1	*knox1-1*	1st exon	GGTGCTTT (***Tnt1***) TGGAGAAA
KNOX1	*knox1-2*	4th exon	TCATCCAC (***Tnt1***) ACTATTAC
KNOX2	*knox2-1*	1st exon	GAAGCTAT (***Tnt1***) AAAAGCCA
KNOX2	*knox2-2*	1st exon	TGTCAAAA (***Tnt1***) GGTCACTA
KNOX6	*knox6-1*	3rd exon	AAAGTGCA (***Tnt1***) GCTTTTAC
KNOX6	*knox6-2*	3rd exon	CTTTTACG (***Tnt1***) CAAGTATA
KNOX6	*knox6-3*	4th exon	GTCATGTG (***Tnt1***) CAAGCCAT

Supplemental Table 2. List of the Number of Transgenic Lines

Transgene name	Background	Species	Number of transgenic lines (T0)
PHANRNAi	Wild type	*M. truncatula*	9
PHANpro:PHAN	*phan* mutant	*M. truncatula*	4
35S:KNOX1	Wild type	*M. truncatula*	14
35S:KNOX2	Wild type	*M. truncatula*	21
35S:KNOX4	Wild type	*M. truncatula*	12
35S:KNOX6	Wild type	*M. truncatula*	11
35S:SGL1	Wild type	*M. truncatula*	21
35S:PHAN	*as1* mutant	*Arabidopsis*	37
35S:PHAN	Wild type	*M. truncatula*	24

T0: First generation transgenic plants derived from tissue culture.

15

Supplemental Table 3. Primers Used in This Study

Primer	Sequence	Application
PHAN-CDS-F	CACCATGTCGGATATGAAAGATAGG	For cloning of the *PHAN* full length CDS
PHAN-CDS-R	CTATCTTCCATTTGATTCAGCATGC	
PHAN-Prom-F	CACCAGCCTACATACTCTAATACATGG	For cloning of the *PHAN* promoter
PHAN-Prom-R	ATCCGACATCCGGTTTCTTGAAAC	
PHAN-Prom-F	CACCAGCCTACATACTCTAATACATGG	For making complementation construct
PHAN-R1	TGCAAAGTCCTCAAGTTGTATG	
$PHAN_{RNAi}$-F	CACCATGTCGGATATGAAAGATAGG	For making $PHAN_{RNAi}$ construct
$PHAN_{RNAi}$-R	GTACTTGCTATCGTTAATCGGGTCG	
KNOX1-CDS-F	CACCATGGAGGGTAGTTCTAATGGAAGTTGTTC	For cloning of the *KNOX1* CDS
KNOX1-CDS-R	CTAGAGCATGGTGTTAGATAGATCCATGGGAT	
KNOX2-CDS-F	CACCATGGAGGAATACACTAATAATCC	For cloning of the *KNOX2* CDS
KNOX2-CDS-R	TCATGGCCCTAAACGGTAGGGAC	
KNOX4-CDS-F	CACCATGCAAGAACCAAGCTTAGGGATG	For cloning of the *KNOX4* CDS
KNOX4-CDS-R	TTACTACCTCTTGCGTTTCGACTTC	
KNOX6-CDS-F	CACCATGTTAGGGTTTGGAGGAAACAGTTGC	For cloning of the *KNOX6* CDS
KNOX6-CDS-R	AGGATTAATGTTCTAAAGAAGCATAGGCATG	
SGL1-CDS-F	CACCATTGCTTACCATGGATC	For cloning of the *SGL1* CDS
SGL1-CDS-R	TAACTTAAAAAGGAAGGTGAGCAG	
PHAN-qRT1-F	CCAGTACGAGGTCCGGACAA	For qRT-PCR analysis of *PHAN*
PHAN-qRT1-R	CAGCGCCATGTGGAGCTA	
PHAN-qRT2-F	AAGAGAGACAGACATCACTTTCAGC	For qRT-PCR analysis of *PHAN*
PHAN-qRT2-R	CAAAGAACAAAAACTAACAAGGACC	
KNOX1-qRT1-F	ATTCATTCAATGGAGGGTAGTTC	For qRT-PCR analysis of *KNOX1*
KNOX1-qRT1-R	AAAGCACCCATCACATAAGAAC	
KNOX1-qRT2-F	CAAGGTTAGAAGAAGCATGTGCAA	For qRT-PCR analysis of *KNOX1*
KNOX1-qRT2-R	CAACCTGATCCAACTGCATCTC	
KNOX2-qRT1-F	CACTACCCAGCTTTAATGAGAAC	For qRT-PCR analysis of *KNOX2*
KNOX2-qRT1-R	ATTAGAACTGCTAGGACTCCCTC	
KNOX2-qRT2-F	GAGTTGCATTACAAATGGCCATAT	For qRT-PCR analysis of *KNOX2*
KNOX2-qRT2-R	ACCTGTTGACTCAGCCAATGCT	

16

KNOX3-qRT-F	TGTGGCGTGTTTGAGGATAGC	For qRT-PCR analysis of *KNOX3*
KNOX3-qRT-R	CTGTGCATCAATCCTCGGTAAC	
KNOX4-qRT-F	TGAAAGGTCACTCATGGAACGA	For qRT-PCR analysis of *KNOX4*
KNOX4-qRT-R	TTCTCGACTTAAAACCCTGTTTGA	
KNOX5-qRT-F	GGTCAATGGCTCTCTCGTCCTA	For qRT-PCR analysis of *KNOX5*
KNOX5-qRT-R	GGTGACGTCGTCGATGACTTC	
KNOX6-qRT1-F	TGGAGGCATATTGTGAGATGCTT	For qRT-PCR analysis of *KNOX6*
KNOX6-qRT1-R	TGGCTTCTTTGAAGGGTTTAGTG	
KNOX6-qRT2-F	TTGGTGGAGCAGGCATTACA	For qRT-PCR analysis of *KNOX6*
KNOX6-qRT2-R	AAGGGCTTGCTTTTGGGATT	
KNOX7-qRT-F	CCTGATGACACCGGAGAATCTAA	For qRT-PCR analysis of *KNOX7*
KNOX7-qRT-R	TGGTGGACATGAGGAAACTGTT	
KNOX8-qRT-F	CATCCGATTACAACCGTTCAGAT	For qRT-PCR analysis of *KNOX8*
KNOX8-qRT-R	CCTTTCCACAACTCATTTCATCCT	
BP-qRT-F	CCATTCAGGAAGCAATGGAGTT	For qRT-PCR analysis of *BP*
BP-qRT-R	ACTCTTCCCATCAGGATTGTTGA	
PHAN-Prob-F	AAGAATTACCTCAAGCCCGGCA	For cloning of *PHAN* as probe for in situ hybridization
PHAN-Prob-R	AGCAACAGCTTGTTCCTCCCTT	
KNOX1-Prob-F	ACCAAGTGAAGTGGTGGCAA	For cloning of *KNOX1* as probe for in situ hybridization
KNOX1-Prob-R	TCCAGTGCCGTTTCCTTTGA	
KNOX2-Prob-F	AAGTGGTGGCTCGTTTGGTT	For cloning of *KNOX2* as probe for in situ hybridization
KNOX2-Prob-R	ATGCAGTCCATCCATCACCA	
KNOX6-Prob-F	TTGCTTGAAGGTTGGAGCACCT	For cloning of *KNOX6* as probe for in situ hybridization
KNOX6-Prob-R	TCCATAGGGAATGGCTTGCACA	
KNOX7-Prob-F	GACAAATCCCTGATGACA	For cloning of *KNOX7* as probe for in situ hybridization
KNOX7-Prob-R	CTTAGCCAGTTCAATCTTAT	
YABBY1-qRT-F	GCGGTTAGTGTTCCATGCAGTA	For qRT-PCR analysis of *YABBY-Medtr4g101660*
YABBY1-qRT-R	GCAAATTAGCACAATGACCACATC	
YABBY2-qRT-F	TGATTGCAACAGAACGTGTTTG	For qRT-PCR analysis of *YABBY-Medtr4g114730*
YABBY2-qRT-R	TGGAACATTAACCGCTAGAATGG	
YABBY3-qRT-F	TGCGTTCTGCACCAACCA	For qRT-PCR analysis of *YABBY-Medtr4g050300*
YABBY3-qRT-R	CGGGAGGGCGGTTAACA	
YABBY4-qRT-F	ATCGGTTGTATGCTGAGGGAACT	For qRT-PCR analysis of *YABBY-Medtr2g087740*
YABBY4-qRT-R	ACGCCCACCAATCATAAACAG	
YABBY5-qRT-F	TCGGACTTATGCCTGATCATCA	For qRT-PCR analysis of *YABBY-*

17

YABBY5-qRT-R	GTCCTCTGAATCCTGACGAACAT	*Medtr4g025900*
YABBY6-qRT-F	ACTCCCAAGTGGACCCCAAT	For qRT-PCR analysis of *YABBY-Medtr5g034030*
YABBY6-qRT-R	CTTCCACGGAATCCTTGTTCTT	
YABBY7-qRT-F	CCATGCAAGAGGCTGCTAGATA	For qRT-PCR analysis of *YABBY-Medtr5g046230*
YABBY7-qRT-R	GAAAAGAGAGGTTGCTGCAGTGA	
REV1-qRT-F	GTTGACTGTTGCCTTCCAGTTTC	For qRT-PCR analysis of *REV1_Medtr2g094520*
REV1-qRT-R	TGCCATGGCTGCAACATTAT	
REV2-qRT-F	CCAGGGATGAGGCCTACAAG	For qRT-PCR analysis of *REV2_Medtr4g058970*
REV2-qRT-R	TGTGTTCCCAAGAGGCATGA	
PHB/PHV-qRT-F	ATGCTGCTGCAGAATGTTCCT	For qRT-PCR analysis of *PHB/PHV_Medtr2g030130*
PHB/PHV-qRT-R	TTCTGATCGATGCTCCCTCAA	
HB8-qRT-F	TCAGCAGCATCCACAACCAA	For qRT-PCR analysis of *HB8_Medtr3g109800*
HB8-qRT-F	AGTCTCCTCTGCAATGGACAAAA	
CNA1-qRT-F	GGCCAACAACCCAAATCG	For qRT-PCR analysis of *CNA1_Medtr2g101190*
CNA1-qRT-R	CCAGCGGGACCAATATCAAG	
CNA2-qRT-F	CAATGGTGCTGGCTCAGAAG	For qRT-PCR analysis of *CNA2_Medtr8g013980*
CNA2-qRT-R	TGCGAAATCTGCCTTAGATGAC	

18